journal of the American Ceramic Society

Consolidation and high-temperature properties of ceramics in the TaC–NbC system

Journal:	*Journal of the American Ceramic Society*
Manuscript ID	JACERS-49016.R1
Manuscript Type:	Research Article
Date Submitted by the Author:	n/a
Complete List of Authors:	Demirskyi, Dmytro; Tohoku Daigaku Zairyo Kagaku Koto Kenkyujo Nishimura, Toshiyuki; National Institute for Materials Science, Nano Ceramics Center Suzuki, Tohru; National Institute for Materials Science, Research Center for Functional Materials Yoshimi, Kyosuke; Tohoku University, Department of Materials Science and Engineering VASYLKIV, Oleg; National Institute for Materials Science, Research Center for Functional Materials;
Keywords:	strength, carbides, hardness, toughness, solid solutions
Author-supplied Keyword: If there is one additional keyword you would like to include that was not on the list, please add it below::	

Consolidation and high-temperature properties of ceramics in the TaC–NbC system

D. Demirskyi (a,b,c)†, T. Nishimura (b), T.S. Suzuki(b), K. Yoshimi (c), O. Vasylkiv (b)†.
(a) WPI-Advanced Institute for Materials Research (WPI-AIMR), Tohoku University, 2-1-1 Katahira, Aoba-ku, Sendai, 980-8577 Japan
(b) National Institute for Materials Science, 1-2-1 Sengen, Tsukuba, Ibaraki 305-0047, Japan
(c) Department of Materials Science and Engineering, Tohoku University, 6-6-02 Aramaki Aza Aoba, Sendai, 980-8579, Japan

Abstract

In this study, we explored the consolidation, solid-solution formation and high-temperature properties of carbides in the Ta–Nb–C system. Tantalum niobium carbide bulks can be consolidated by spark-plasma sintering only at a temperature of 2200 °C using a 30-min dwell. The ceramics were homogeneous solid solutions and a linear dependence of the lattice parameters on the NbC content was observed. The average grain size varied between 10 and 30 μm, while the reference monolithic tantalum carbide consolidated under similar conditions had a grain size exceeding 40 μm. The room temperature strength linearly decreased from TaC to NbC. The 75 mol.% NbC ceramic showed almost an unchanged strength up to 1600 °C (450±20 MPa), following the linear decrease in strength to 290 MPa at 2000 °C. The monolithic tantalum carbide had showed the lowest strength at 2000 °C among the studied ceramics.

† Authors to whom correspondence should be addressed, Dmytro Demirskyi, demirskyi.dmytro.e2@tohoku.ac.jp, Oleg Vasylkiv oleg.vasylkiv@nims.go.jp

Keywords: solid solutions; strength; carbides; hardness; toughness.

1. Introduction

It is well established that carbides of the refractory metals, such as Ta, Nb, Zr or Hf, are the backbone of the ultra-high temperature ceramics (UHTC) family. These carbides have a high-hardness, elastic moduli and melting points due to a mixed ionic-covalent, metallic-ionic bonding inside a rock-salt type cubic cell [1,2]. Due to their high-melting points [3], UHTC carbides are extremely difficult to densify [4]. The activation of diffusion in these ceramic carbides requires temperatures exceeding 2000 °C. Tantalum carbide, in particular, is difficult to densify to full density, and even application of advanced processing methods, such as hot-pressing or spark-plasma sintering (SPS), results in noticeable grain-growth [5,6].

Because of a direct dependence between the grain size and strength, and porosity and Young's modulus, one prefers to achieve both fine grain size and pore-free samples in order to form a ceramic with a maximum performance. The main advantage of these carbide is their high stiffness as Young's modulus for the bulk tantalum carbide and niobium carbide is 558 GPa and 537 GPa, respectively. In particular tantalum carbide is an emerging material for use in the propulsion sector, where the environment is reducing, so the pesting oxidation featuring these carbides is not the main issue. On the contrary, thermal shock resistance and low damage

tolerance are two impelling problems [7,8]. In this respect, the formation of the solid-solution can be considered as one of the methods for improving the fracture toughness of monolithic TaC or TaC-based ceramics.

Nevertheless, the main task remains to consolidate the fully dense carbides to achieve a maximum in the performance. One can promote consolidation in UHTC carbides by using a small amount of various additives [8–10]. However, the mechanical properties will be dependent on the ability of these additives to withstand deformation or form coherent interfaces with the carbide [8]. An alternative route to processing would be optimization of the processing such as using a fine powder or promotion of a solid-solution reaction [11,12]. In ref. [12], it was reported that solid solution ceramics in the TaC–NbC system show a good creep resistance at 2550–3100 °C for the NbC-rich compositions, while ref. [13] reported that the proof stress in the TaC–NbC ceramics during creep in flexure at 2800 °C would linearly decrease from the bulk TaC to bulk NbC.

TaC and NbC share the rock-salt lattice and, hence, it is assumed that these carbides will have an unlimited solubility in each other [1,2]. Diffusion of carbon in NbC and TaC was studied by Rafaja et al. [14,15] and Andrievski et al. [16]. These studies were performed at different temperatures. However, results indicate that carbon will diffuse in NbC faster that in TaC (*see Supl. S1*). Other results on the diffusivity in UHTC carbides are summarized by Matzke [17], or Andrievski [2].

Because of a significant interest being recently focused on solid-solutions in general [18–20], and to the 'high-entropy carbide' family in particular [21–23], we consider that fundamental research on the binary UHTC carbides would promote our understanding of the carbide processing and will allow us to engineer ceramics with predefined properties. It is noteworthy that theoretical predictions on the binary system for the same transition metal group may lead to the formation of an unstable solid-solution or the system may experience a limited solubility in a selected temperature range [24]. Hence, within this study, we focused our attention on the carbides in the TaC–NbC system. Thus, the preparation and analysis of the solid-solution between tantalum and niobium carbide is the main goal of this study. In order to form the tantalum niobium carbide bulks the spark-plasma sintering was performed at a temperature of 2200 °C. Furthermore, this study aims to analyze data regarding the lattice parameters, hardness, toughness and high-temperature mechanical strength using the three-point flexural strength method.

2 Materials and Methods

Commercially-available TaC (Lot #LKP4101) and NbC (Lot #W19E52) by Wako Pure Chemical Industries were used as the starting materials (*see Supl. S2*). The received untreated powders were used for consolidation by the SPS method at various molar ratios between TaC and NbC (**Table 1**). The SPS experiments were

conducted using the 'Dr. Sinter' 1050 (Sumitomo, Japan) unit with a 30-mm die, and as a rule, 32 to 45 g batches were produced.

The schedule for the carbide specimens prepared in this study had four major steps: (1) heating to 700 °C with a rate 170 °C/min and (2) a 500 °C/min heating to the densification temperature within 2200 °C. At 2200 °C, then a dwell of 30 min was used as a homogenizing step. The final step included cooling to 600 °C in 40 minutes. The pressure of 34 kN was maintained during the consolidation and cooling stages. Argon gas at the flow rate of 2 L/min was used.

An X-ray diffraction (XRD) analysis (D8 Advance, Bruker, Karlsruhe, Germany) was performed on the polished surfaces of the bars after the flexural tests using Cu-Kα radiation. The intensity data were collected over the 2θ range of 30°–145° in steps of 0.02° using a sampling time of 10 s for each step. The software used for refinement was TOPAS (TOPAS Ver. 4.2, Bruker AXS, Germany). Instrumental broadening was determined using a NIST 660b LaB_6 standard run under the same conditions for each carbide sample.

The structural characteristics of the carbide ceramics were studied by scanning electron microscopy (SEM, JCM-6000, JEOL) with secondary (SE) or backscattered electrons (BSE mode).

Bulk density of hot pressed specimens was measured by Archimedes' method using distilled water as the immersing medium according to ASTM B 311-17 or ASTM B

962–08. The average and median size that were quantitatively measured by an intercept technique, using (π/2) as a constant [25]. At least 200 grains were measured at magnifications ranging from ×200 to ×1000 (*see Supl. S3*). Porosity was evaluated using polished SEM images using Fiji software [26] (*see Supl. 4*).

The three-point flexural strength was determined using rectangular blocks (1.5×2×25 mm, AS TM C1211−13, configuration A) and the strength testing equipment that was previously described in detail [27]. A span of 16 mm was used. The fracture toughness of the ceramics was evaluated by the specimen bending testing which contained a single edge through-thickness notch following ASTM C1421–10 (single edge through-thickness notch 3 mm×4 mm×25 mm, notch width 90 μm, depth 0.4–0.6 mm, a0/W <0.15). The toughness was tested in the same direction as the pressure was applied during the SPS consolidation. Details of the testing configuration and the notch profile were presented in ref. [28]. At least two measurements were performed at the loading speed of 0.5 mm/min. The flexural strength data were averaged based on three tests at the elevated temperature and by five tests at room temperature.

The hardness was determined by an MMT-7 Vickers hardness tester (Matsuzawa MMT-7; Matsuzawa SEIKI Co., Ltd., Tokyo, Japan) using loads of 49 N and 98 N with a dwell time of 15 s following the standard procedure (ASTM C 1327–15).

Over 20 measurements at different locations were conducted for each specimen at each indentation load to ensure the statistical validity of the hardness data.

3 Results & discussion

3.1 Consolidation and phase formation

Figure 1 shows details of the non-isothermal runs of the selected mixtures at the heating rate of 500 °C/min and the constant pressure of 34 kN. It can be seen that a noticeable shrinkage was observed above 2000 °C, however, the shrinkage for the 50 mol.% NbC solid-solution was the highest observed for all the attempted mixtures. This composition had the finest grain size after a non-isothermal run to 2200 °C, and also after a 30-min dwell: 5.6±0.8 μm and 17.3±7.9 μm (**Table 2**), respectively. Following the non-isothermal runs, the relative density of the bulks remained below 85–92% of the theoretical density evaluated by the XRD data. Analysis of the isothermal runs showed that monolithic tantalum carbide had a different densification behavior, while other specimens were densified using diffusion-based sintering mechanism(s) (*see Supl. S5*).

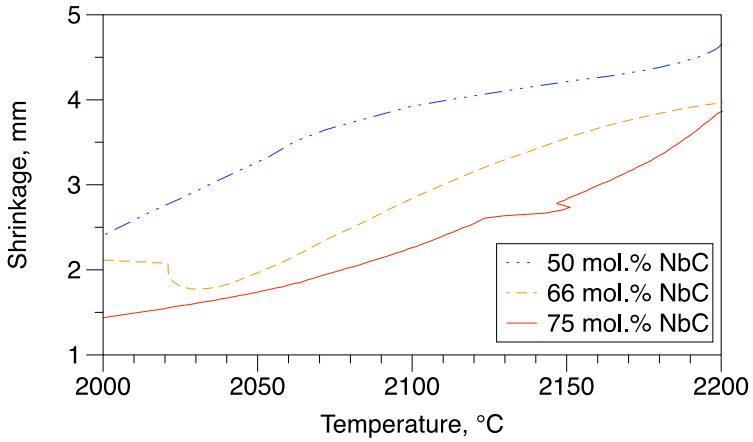

Figure 1. Shrinkage behavior of the powder compacts at the heating rate of 500 °C/min and the constant pressure of 34 kN.

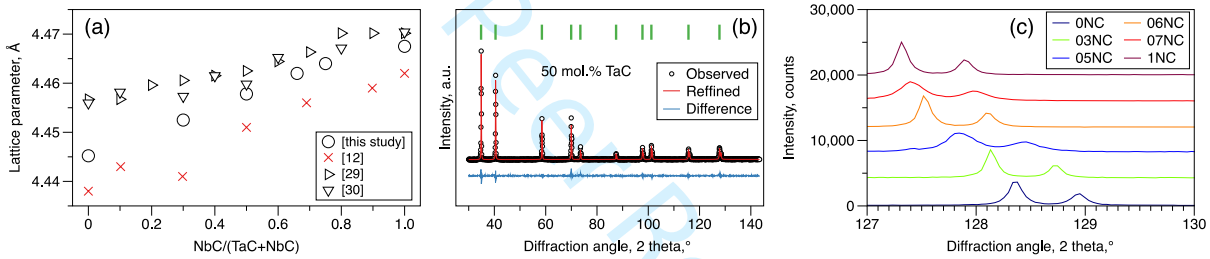

Figure 2. The lattice constant of the solid-solution carbides in the TaC–NbC system as a function of the NbC content [12,29,30]. (b) shows the refinement of the equimolar ceramic using the lattice parameter of 4.457(8) Å. (c) shows peak shift for all compositions in the TaC–NbC system.

Figure 2 shows the lattice constant of the solid-solution carbides in the TaC–NbC obtained within this study and in refs. [11,22,23]. First, the lattice parameters of the SPSed carbides differ by 0.5%, and those of the solid solution closely follow Vegard's law from 4.445 Å (bulk TaC) to 4.467 Å (bulk NbC) (*see Supl. S6*). Second, there is a slight deviation in the value for the lattice constant of the cubic

phase can be seen while comparing the three data sets. One can presume that such a deviation may be due for different impurities in the raw powders as well as a carbon deficiency in the carbide lattice. For the latter case, the studies of Bowman et al. [31] and Storms et al. [32] provide the wide data for the TaC_x and NbC_x phases, respectively. These data are illustrated in **Figure 3**, where the dashed lines indicate the findings for the monolithic TaC and NbC bulks after the SPS. Assuming a linear approximation, one can derive that the tantalum carbide with the chemical formulas of $TaC_{0.93}$, $TaC_{0.84}$, and $TaC_{0.98}$ were used in this study based on Katz et al. [12] and Norton et al. [29], respectively. For the niobium carbide, the same treatment of the data in **Figs. 2** and **3** yields the composition $NbC_{0.93}$, $NbC_{0.88}$ and $NbC_{0.97}$ for this study.

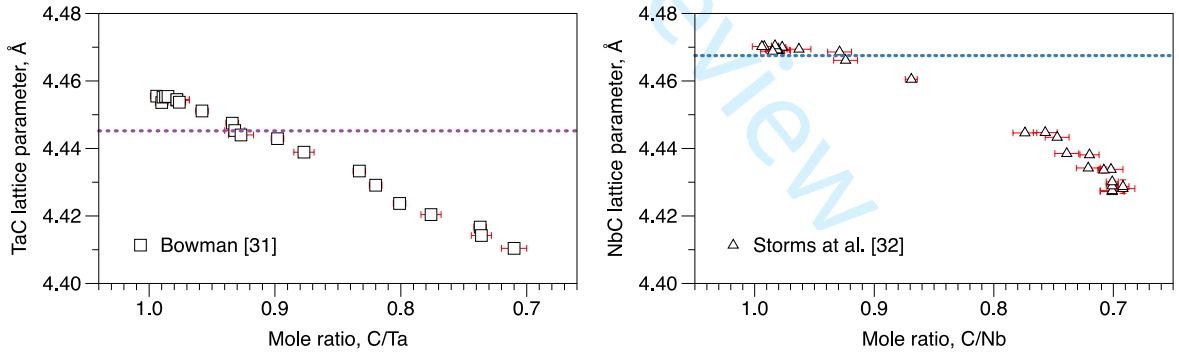

Figure 3. The lattice constant of the TaC and NbC as a function of the C to metal ratio [31, 32]. Dash line is for the lattice parameter of TaC and NbC bulks after the SPS consolidation.

One should treat these data quite carefully as the carbon deficiency in the carbide controls the hardness as it directly correlates with the amount and strength of the metal-ionic and covalent-ionic bonds in the lattice [1]. Furthermore, after the consolidation, it is common for carbides to have a free or unbonded carbon in the final structure [1]. In such a case, the total chemical ratio between the carbon and metal may approach unity as would the specification from the powder manufacturer may suggests. Other non-metals, such as N or O, may also influence the lattice parameter of the carbide, however, these are mostly related to the ZrC or HfC ceramics due to the higher attraction of the metallic Zr or Hf to bonding with the oxygen [1]. In this study, for the monolithic TaC and NbC carbides, the main impurities measured by laser spectroscopy were TaC (Al 0.07 wt.%, O <0.15 wt.%, Cr ≲0.1 wt.%, Nb < 0.3 wt.%) and NbC (Fe <0.3 wt.%, O <0.5 wt.%, Ta <0.6 wt.%, Ti <0.1 wt.%).

Figure 4 shows the microstructure of the ceramic after spark plasma sintering at 2220 °C. These images were obtained using the BSE mode. They show the formation of a homogeneous solid solution. The contrast in color for monolithic tantalum carbide is due to the fact that different crystallographic faces were scanned with an electron detector (i.e., the color will shift for the same grain as the image shifts).

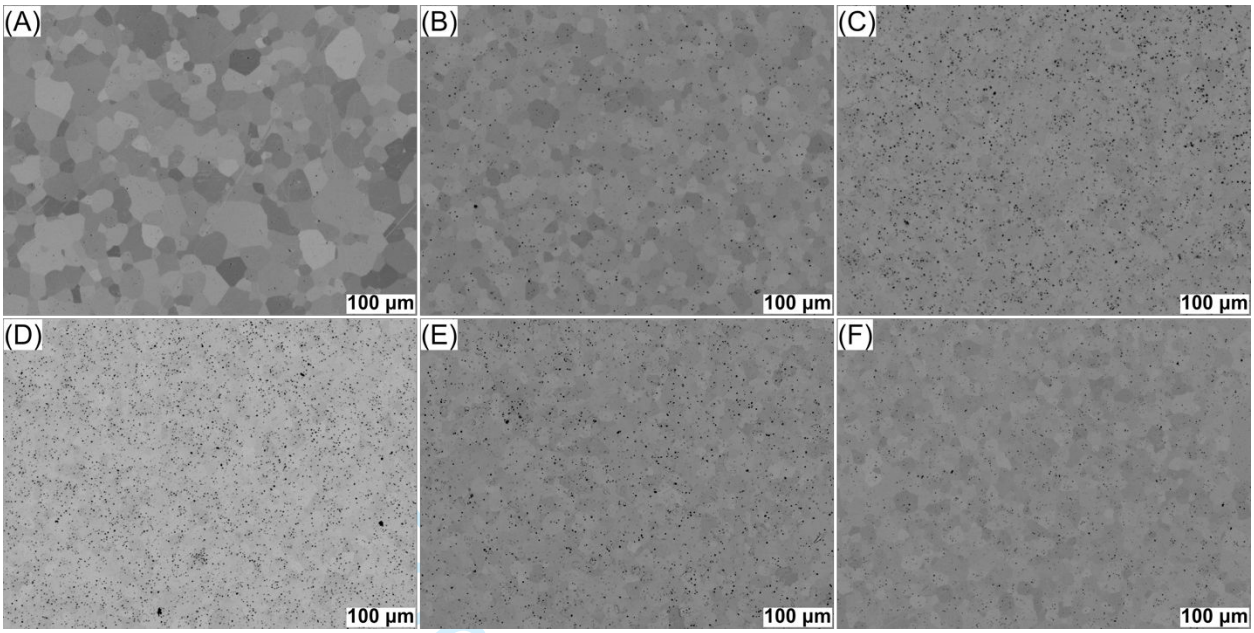

Figure 4. Representative microstructure of ceramics in the TaC–NbC system after SPS: a) 0NC b) 03NC, c) 05NC, d) 06NC, e) 07NC, and f) 1NC.

3.2 Hardness in the NbC–TaC system

The results of the hardness measurements are summarized in **Figure 5**. One can see that we observed the local maxima at the 66 mol.% or 75 mol.% NbC composition exceeding the values for individual carbides or an equimolar solid-solution. These observations were made using 49 N or 98 N loads. However, we should underline that the hardness data had a maximum of standard deviation of ±0.8 GPa, and similar to the lattice parameter the linear increase in the hardness was observed.

A further increase in the load during the indentation tests resulted in numerous cracks and the shape of the indent did not agree with the regulations imposed by ASTM

C1327–15. Contrary to the first-principles calculations [24], the hardness of the monolithic NbC bulks was higher than that for TaC. A similar result can be found in refs. [33, 34] as the microhardness of NbC and TaC was estimated to be 18 and 16 GPa, respectively.

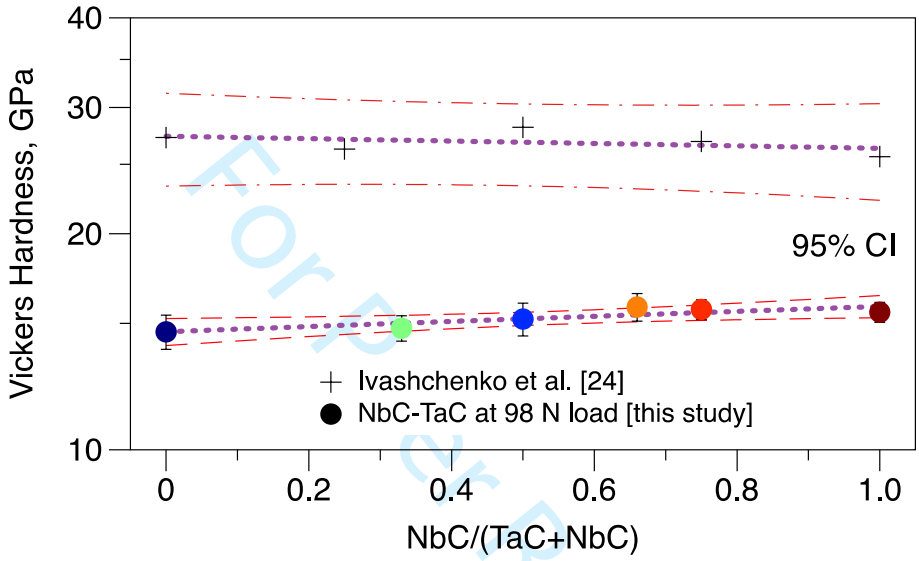

Figure 5. Hardness in the TaC–NbC as a function of the NbC content and hardness data according to the first-principles calculations in ref. [24]. Dashed lines indicate the 95% confidence intervals for the regression line.

3.3 Toughness in the NbC–TaC system

To the best of author's knowledge, only the studies of Gridneva et al. [35] and Grigor'ev et al. [36] reported the toughness of NbC and the value varied from 2.8 to 3.8 MPa $m^{1/2}$ (**Fig. 5**) [6,8,20,33–38]. In ref. [35], with an increase in the temperature, it was reported that the toughness of niobium carbide decreased to

3.2 MPa $m^{1/2}$ (500 °C) or 1.8–2.0 MPa $m^{1/2}$ (900 °C). These observations were confirmed by Grigor'ev et al. in ref. [36]. The toughness data of tantalum carbide suggest that the toughness below 4.0 MPa $m^{1/2}$ is highly reproducible [8], while ref. [37] reported a toughness of 5.3±0.7 MPa $m^{1/2}$. The maximum toughness measured within the present study was for a 03N composition (4.7±0.2 MPa $m^{1/2}$), while the lowest was for the bulk tantalum carbide (3.1±0.1 MPa $m^{1/2}$).

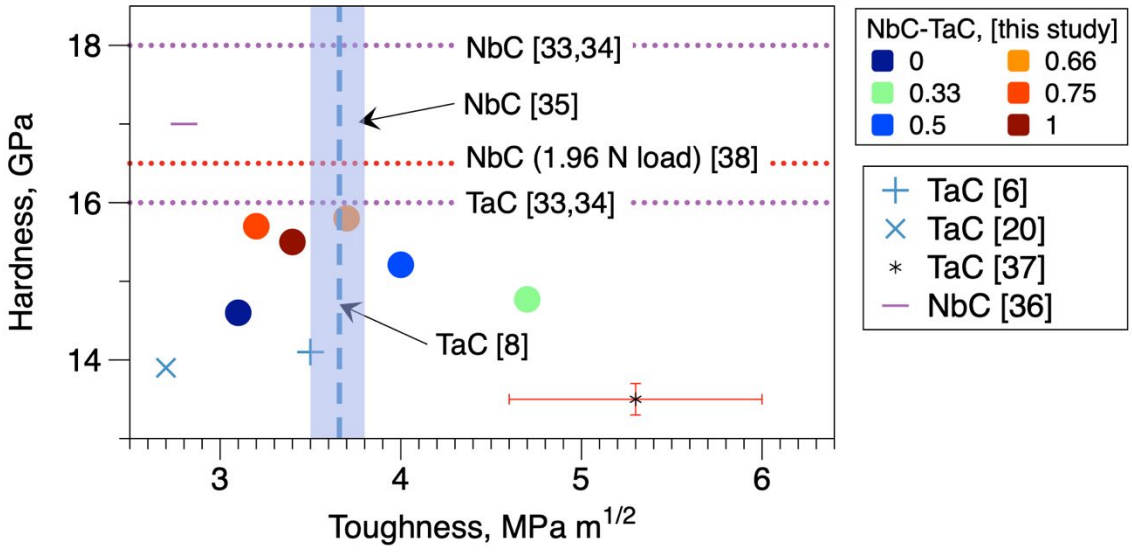

Figure 6. Relation between hardness and fracture toughness in the TaC–NbC system, and for TaC [6,8,20,33,34] and NbC [33–38] bulks. The toughness in [8] was measured by the flexure approach. Horizontal dot lines are for the hardness. Vertical dashed line and shaded area are for the toughness determined in [8] and [35] for TaC and NbC, respectively.

In general, the toughness of the TaC–NbC ceramics can be summarized within a margin of 3.4±0.4 MPa $m^{1/2}$, while only the 05NC and 03NC bulk yielded a

toughness exceeding 4 MPa $m^{1/2}$ (also *see Supl. S7* for TaC). For these ceramics, one may consider that a slight increase in toughness at room temperature can be attributed to the formation of a solid solution between the carbides as was suggested in ref. [22] for the medium-entropy carbide. For the case of the equimolar composition, the toughness was also evaluated using the indentation method [39]. Such efforts yielded a toughness of 4.06±0.72 MPa $m^{1/2}$, confirming the data obtained by flexure. In this study, the most likely sources of increased toughness are strain due to the formation of the solid solution and grain size. Without data on the toughness of samples with identical grain sizes, it is difficult to speculate on the effects of composition on the toughness of the carbides in the TaC–NbC system.

3.4 Flexural strength in the NbC–TaC system

First, the data obtained in other studies on monolithic tantalum and niobium carbides will be discussed and compared with the results obtained in this study for 0NC and 1NC samples. Then, the analysis of the bending strength for solid solutions in the NbC-TaC system will be presented.

3.4.1 Strength data for monolithic TaC

The high-temperature flexural behavior of tantalum carbide is summarized in the **Fig. 7** [9,40–43]. A study [9] reported a deep minimum at 1400 °C followed by an

increase in the strength. This was not explained in ref. [9], but it is most likely connected with the plasticity contribution. Above 1600 °C, it is known to possess a strength below 200 MPa. The data for the brittle to ductile transition temperature (BDTT) of tantalum carbide showed quite a wide range from 1550 °C to 2300 °C [42,44,45].

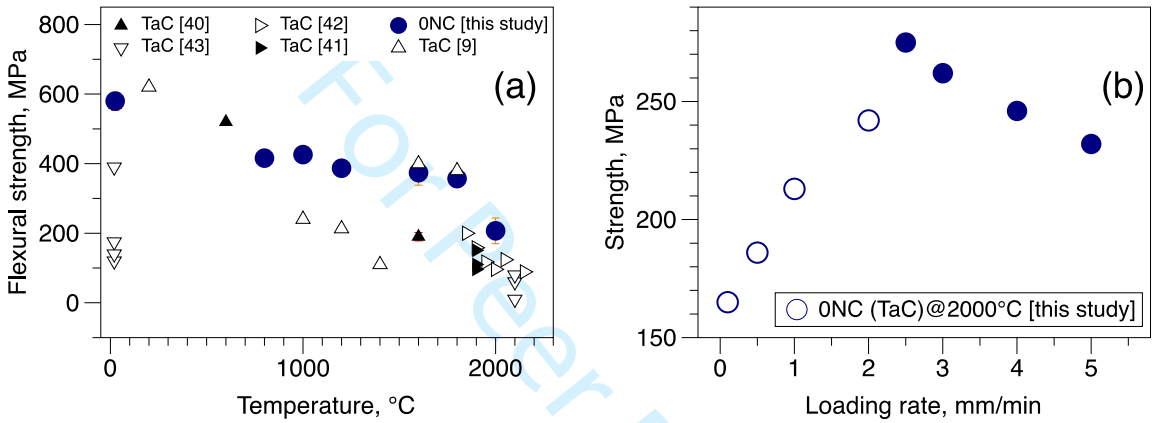

Figure 7. Temperature dependence of the flexural strength of bulk TaC [7,40–43]. (b) effect of the loading rate on the flexural strength at 2000 °C. Open circles in (b) indicate that the specimens were not tested until fracture at these loading rates.

Similar to the flexural strength, the BDTT is sensitive to a carbon deficiency [45], method of fracture, consolidation or annealing conditions, and strain rates [44]. In this respect, the flexural strength observed within this study can be explained as follows: there is a slight decrease in strength between 800–1200 °C compared to that at room temperature. Such a decrease in strength is due to the partial relaxation of the thermal stresses upon reheating. Within 1600–1800 °C, both the strength and

elastic modulus decrease by 10%. A quasi-monotonous decrease in the modulus suggests that BDTT was not reached. At 2000 °C, there is sharp decrease in the strength and modulus (30–40%), and the strength becomes quite sensitive to the loading rate (strain rate). These observations suggests that the BDTT for the tantalum carbide consolidated within this study should be in the vicinity of 2000 °C. As can be seen from the fracture behavior **(Fig. 8)** some quasi-brittle fracture can be still identified at 2000 °C, however, similar to the findings for HfC [46], such a fracture behavior can be only observed for the grains with size exceeding 40 μm. Finer grains would fracture according to the intergranular fracture mechanism.

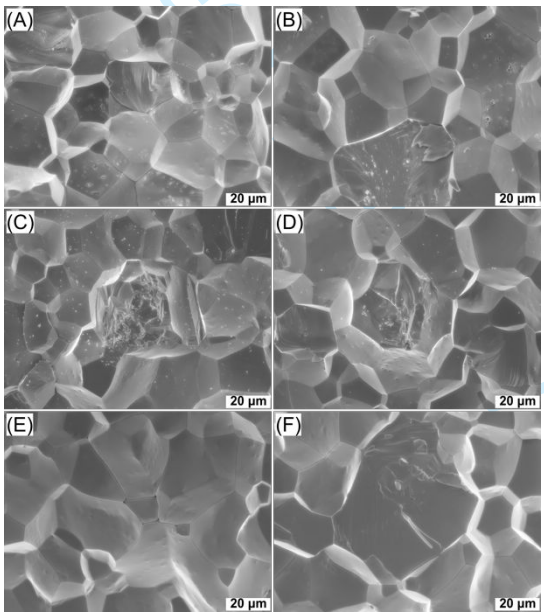

Figure 8. Effect of temperature of the flexural test on the fracture behavior of the monolithic tantalum carbide. (a,b) 800 °C; (c,d) 1600°C, and (e,f) 2000 °C.

3.4.2 Strength data for monolithic NbC

The data for the monolithic niobium carbide bulk is quite diverse [2,35,43,47,48] and were analyzed as a function of the temperature in the study of ref. [49]. In particular, the transition between brittle and ductile fracture is associated with a bell-shaped strength dependence (i.e., with a clear maximum). The peak strength for these ceramics is usually observed in the vicinity of the BDTT. According to the findings of refs. [13,50], a higher consolidation temperature allows shifting of the peak strength (or BDTT) to higher temperatures.

Figure 9 summarizes the data for the mechanical performance of the niobium carbides bulks. For clarity, a typical bell-shaped strength variation vs temperature for the data of ref. [47] was connected using a solid line. The data of the present study follow a shape typical for the temperature dependence of hardness (**Fig. 9 (b)**). Thus one can define two zones: 1) below 1000 °C where the flexural strength varies within the margin of error (or even increases by 10% at 800 °C); and 2) almost a linear decrease in strength up to 2000 °C. The vertical dash line at 1200K is the BDTT according to Grigor'ev et al. [36]. These values were based on the hardness and toughness temperature dependence presented in (**Fig. 9(b)**).

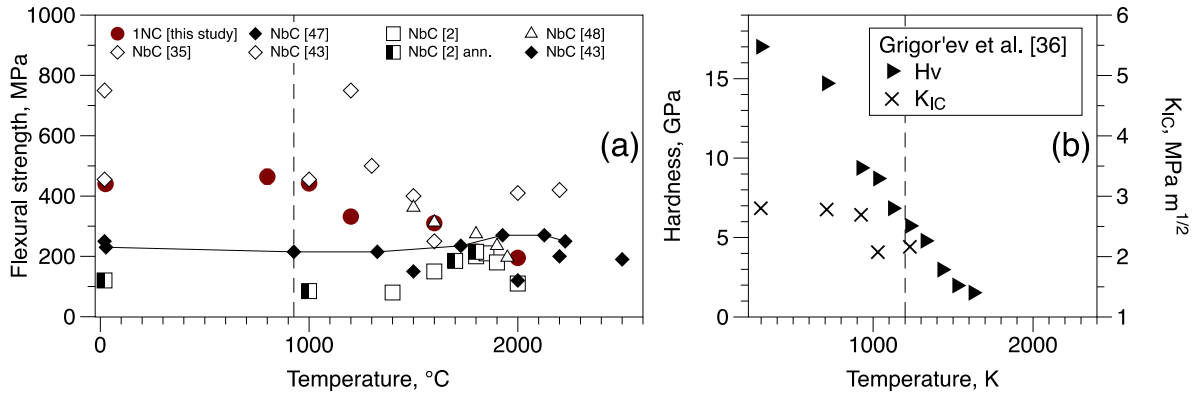

Figure 9. Temperature dependence of mechanical properties of niobium carbide ceramics [2,35,43,47,48]. (a) flexural strength and (b) hardness and toughness for bulk NbC by Grigor'ev et al. [36]. Vertical dash line corresponds to the sharpest maximum in the length of the radial crack observed during the indentation process in ref. [36]. Data from ref. [2] are for annealed and as-consolidated specimens.

Gridneva et al. [35] also studied the temperature dependence of the toughness, strength and microhardness for single-crystalline specimens of niobium carbide. Their results suggested that the BDTT should be around 1200 °C, while the theoretical prediction based on the strength data yielded at least 1500 °C for the polycrystalline niobium carbide. Observation of the fracture behavior suggested that even at 1600 °C a quasi-brittle fracture was observed. The cleavage fracture was along the (100) plane. Sliding was also observed along the (111) <110> slip direction.

In the present study, we could identify the presence of the quasi-brittle fracture at all temperatures for NbC, but at 2000 °C, it was mostly present in the 50–80 μm grains (**Figure 10**). In the low temperature range (**Fig. 11**), fracture for all the attempted ceramics with the exception of the bulk TaC was mainly transgranular. In this temperature range, one can estimate that the critical flaw size would be between 20 and 30 μm which satisfies the general observation that the fracture in the majority of specimens occurred at the expense of the surface flaws.

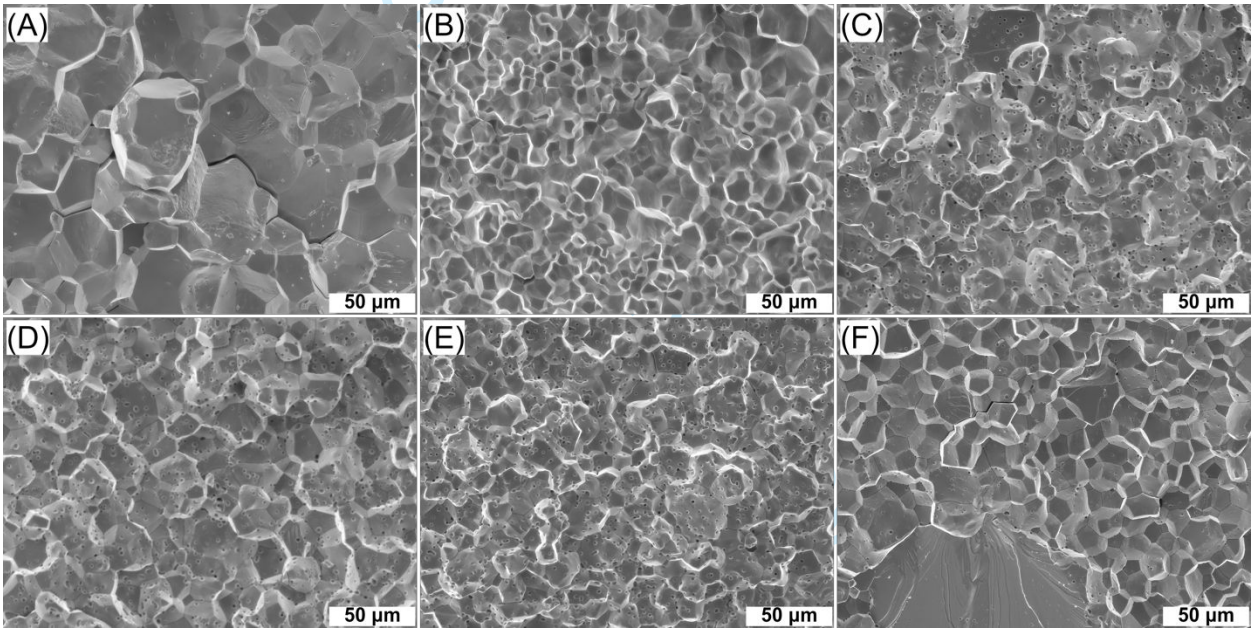

Figure 10. Representative fracture of ceramics in the TaC–NbC system during the flexural strength tests at 2000 °C. a) 0NC, b) 03NC, c) 05NC, d) 06NC, e) 07NC, and f) 1NC.

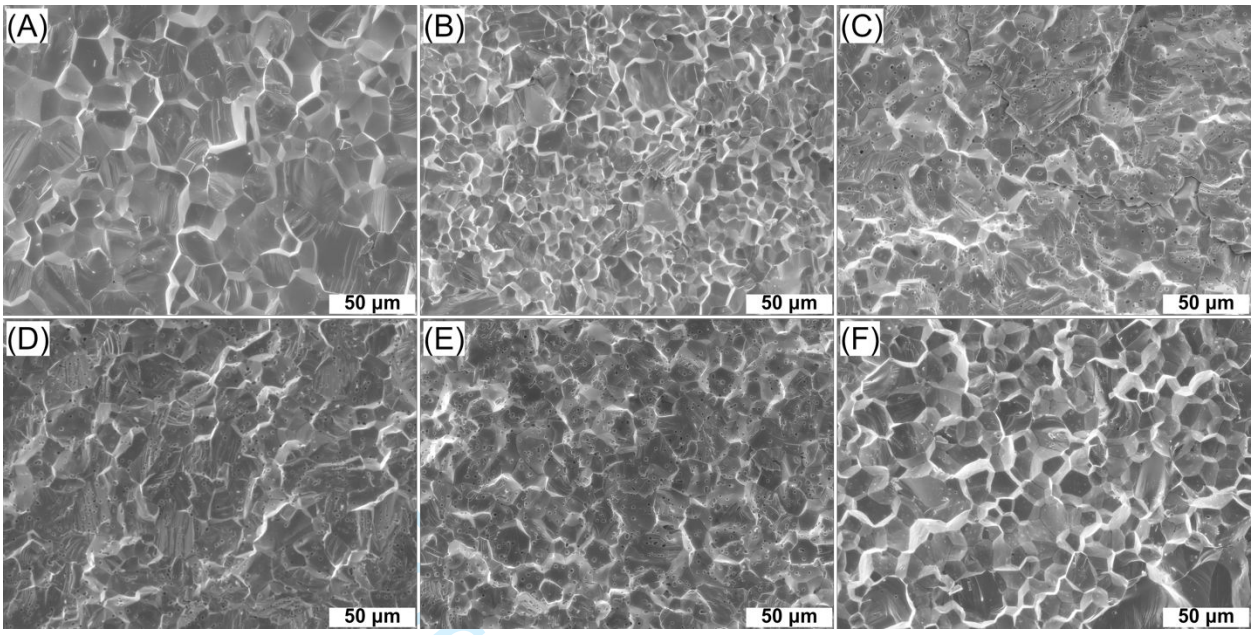

Figure 11. Representative fracture of ceramics in the TaC–NbC system during the flexural strength tests at RT and 800 °C. a) 0NC, b) 03NC, c) 05NC, d) 06NC, e) 07NC, and f) 1NC. a,b,f 800 °C and c,d,e RT.

3.4.3 Strength and fracture of NbC–TaC solid solutions

The strength of the TaC–NbC ceramics as a function of temperature and composition is provided in **Figure 12**. The equimolar composition and 03NC ceramics underwent a monotonous decrease in strength with an increase in temperature. The 06NC ceramic showed an unchanged strength up to 1000 °C followed by a linear strength decrease. The ceramic with 75 mol.% NbC showed an almost unchanged strength up to 1800 °C, but at 2000 °C, the strength decreased to ~400 MPa. For the cubic carbide ceramics, the decrease in strength in the temperature range of 1000 °C–

1400 °C can be directly connected to relaxation of the thermal stresses upon reheating of the ceramic. While the stability to deformation at elevated temperatures can be viewed as the presence of such stresses at elevated temperature, local bonding [13] or the grain size [2]. Coarse grains may allow an increase in the strength at elevated temperatures due to the grain-boundary sliding as was noted by Saunders and Probst for HfC [51]. For such a case, the stress concentrations can be relieved by presenting premature failure and thus allowing higher applied stresses to be reached before fracture.

The flexural strength at a selected temperature can be analyzed as a function of the composition. Such efforts were made for room temperature tests and for the data at 2000 °C (**Figure 12 (b)**). One can see almost a linear strength dependence as a function of the NbC content for the room temperature data. Monolithic tantalum carbide is known to have a strength within 500–600 MPa [6,8], and the reference specimen prepared in this study had a strength of 522±16 MPa. One should keep in mind while analyzing such a linear fit that the data for other parameters that directly influence the strength at room temperature, such as the grain size, the bulk density is different between the tested specimens. The strength data at 2000 °C allows to see that the strength for an equimolar composition and for the 25 mol.% NbC are the lowest within the TaC–NbC system. Note that the previous high-temperature

flexural tests performed on the monolithic TaC in refs. [19,40] showed a strength below 200 MPa.

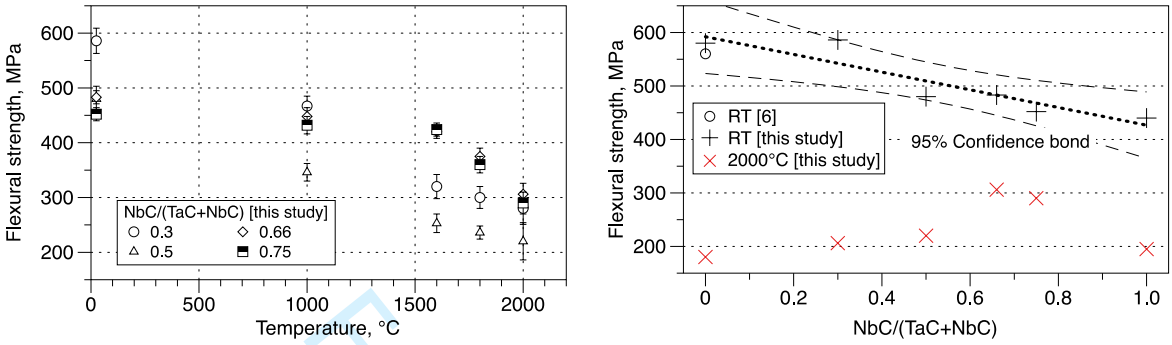

Figure 12. Flexural strength in the TaC–NbC system as a function of the testing temperature and NbC content.

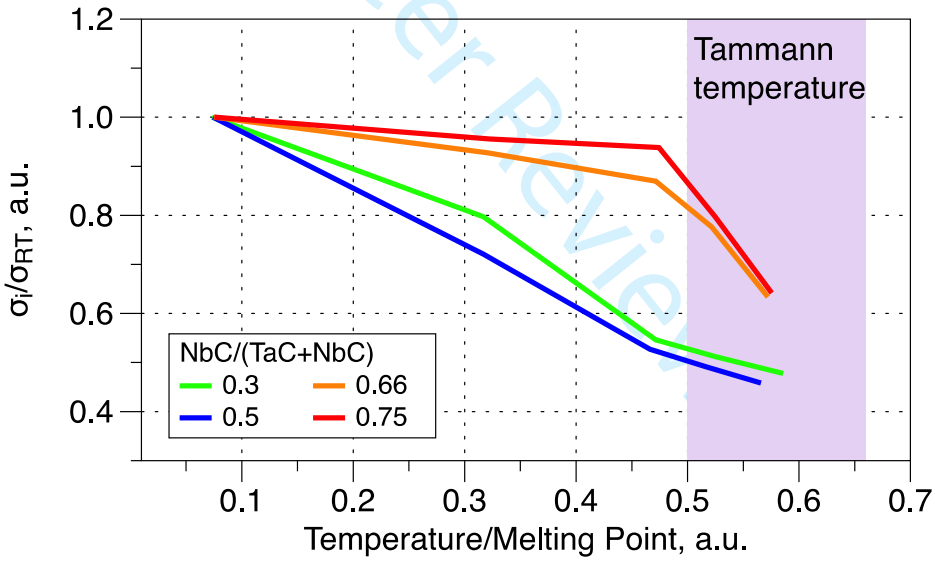

Figure 13. Flexural strength as a function of the homologous temperature and NbC content.

Figure 13 shows the relative strength decrease as a function of the homologous temperature and NbC content in order to clearly illustrate the effect of the

composition on the ability to retain the flexural strength measured at room temperature into the high-temperature zone. The homologous temperature in **Fig. 13** is the relation between the flexural test temperatures and the value of the melting temperature for a selected TaC–NbC using the provisional values of 3880 °C and 3608 °C and assuming a rule of mixtures. The region of the Tammann temperature (~0.5–0.66 Tmelt) is marked here using a purple color. Similar to metals and other UHTC compounds, carbides are expected to experience an enhanced mobility of defects in this temperature range.

One can see that a solid solution in the TaC–NbC system would have a noticeable strength decrease before half of their melting point. It is highly likely that this can be due the finer grain size. Once the strength decrease is due to the activation of the diffusion process during the test, the finer grains will slip more readily and may influence the size of the plastic zone near the crack opening area [13].

Figure 14 illustrates the microstructure of the TaC–NbC bulks after flexural tests at 1600 °C. First, the TaC had the largest grain size. The authors found that the TaC powder is quite easy to sinter, and one can obtain a density exceeding 98% TD at 1500 °C, hence, a finer grain size. However, the flexural strength of such produced bulks would be below 100 MPa at 1600–2000 °C. Hence, for reproducibility, all compositions were soaked at identical temperatures allowing the solid-solution to homogenize. Nevertheless, to the surprise of the authors, the TaC bulks after

2200 °C had almost no visible porosity. The polished samples showed a <0.1 vol.% of extremely fine 0.5–1.0 μm pores (*see Supl. S4*). However, sintering at 2200 °C contributed to a significant increase in grain size.

Second, after reaching the equimolar composition, there was a considerable amount of pores, up to 4 vol.%, and these were predominantly located at the grain-boundaries. Observation of the polished specimens with these compositions suggested that only 20 to 30 % of the pores were located inside the grains. Third, some oxycarbide particles were identified in the 05NC to 1NC compositions (O ~ 3–13 mol.%) (*see Supl. 8*). These were entrapped inside the grains, suggesting that they are the artifacts of the early stages of sintering. In the case of the TaC, it was suggested by Zhang et al. [6] that the small addition of B_4C or C can mitigate the amount of the secondary phases during processing, and result in the minimal grain growth and mostly intergranular porosity. Similar steps may be implemented if the secondary phases are undesirable for creep performance [12].

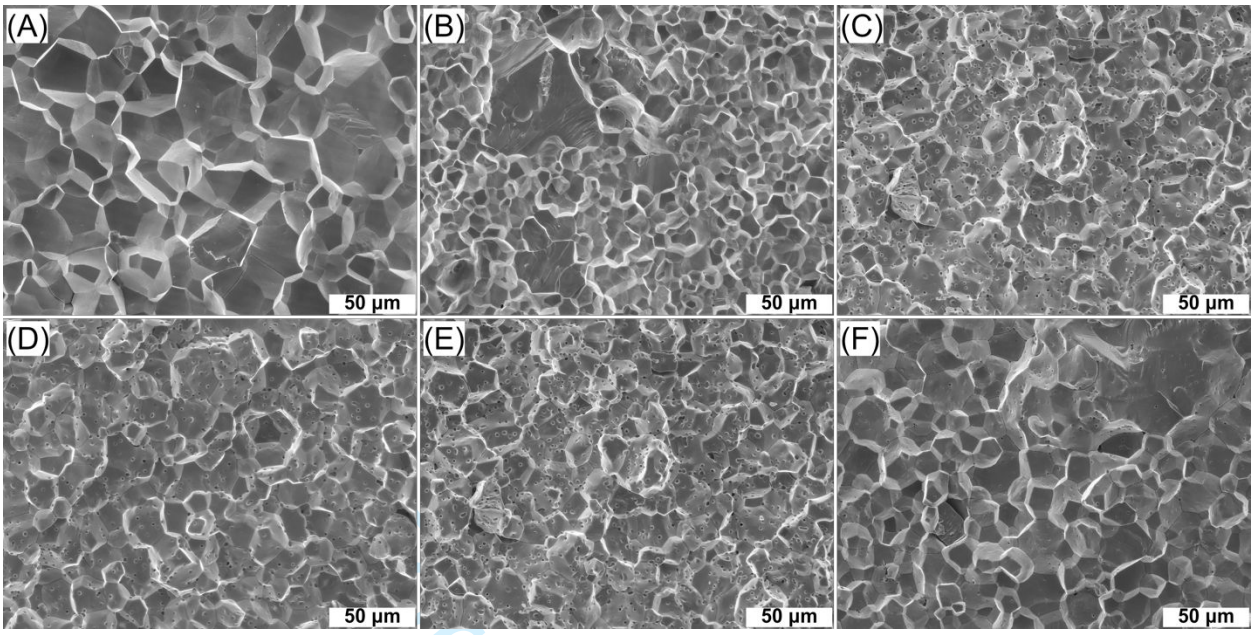

Figure 14. Representative fracture of ceramics in the TaC–NbC system during the flexure at 1600 °C. a) 0NC b) 03NC, c) 05NC, d) 06NC, e) 07NC, and f) 1NC.

Furthermore, one of the main features of the TaC–NbC system is that the majority of oxides should melt below 2000 °C [52–54]. Also, the Ta_2O_5-rich section of the pseudo-binary Ta_2O_5–Nb_2O_5 would be a liquid with Ta_2O_5 above 1600 °C. This should facilitate the reaction between the free-carbon with an oxide at elevated temperatures. As a rule, the majority of oxides would have up to 2–3 wt.% of free carbon. The authors believe that the reaction between the oxide and free carbon can be responsible for the pore-free TaC-rich bulks. It is highly likely that the formation of the fine carbide particles should facilitate sintering [55].

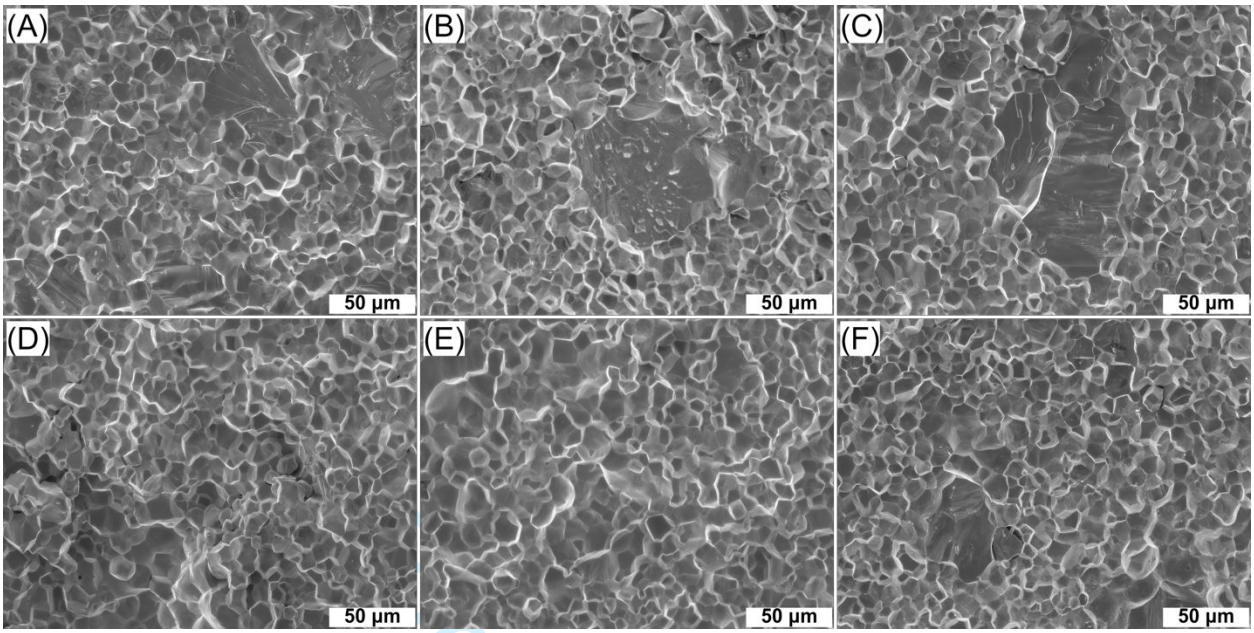

Figure 15. Effect of temperature of the flexural test on the fracture of the 03NC ceramic at (a) 800 °C, (b) 1000 °C, (c) 1200 °C, (d) 1600 °C, (e)1800 °C, and (f) at 2000 °C.

Another observation can be made by observing the fracture behavior as a function of the temperature (**Figs. 15,8**). One can see that the coarse grains had a quasi-transgranular fracture. More noticeably, the pores are absent at the fracture surface while a considerable number of cleavage lines with various orientations to the fracture surface can be observed. With an increase in the temperature such fracture lines become parallel to each other, suggesting that there is a predominant slip-system. The UHTC carbides are known to have a number of possible slip-systems [56], and, for instance, the ZrC [57,58] data indicate that there is a distinctive change

in the slip-system at high-temperatures. For the TaC, at 2300 °C, Smith et al. [59] identified the <110>{110} as the main slip-system. Previous reports about the TaC suggested [60,61] that the <110>{111} should dominate. Hollox summarized that <1-10>{111} <1-10>{110} can be important for the TaC or NbC [41]. Gridneva et al. [35] observed that the cleavage fracture was along the (100) plane for the niobium carbide single-crystals. They reported that the sliding was observed along the (111) <110> slip direction.

Above 1800 °C, the surface of the ceramic grains, in general, becomes smooth while some thermal induced etching pits were seldomly observed. Examples of quasi-transgranular fracture were observed only for the large-sized grains (03NC) similar to the lower temperature tests, for the elevated temperatures several dominant slip systems can active [1,2,13,57].

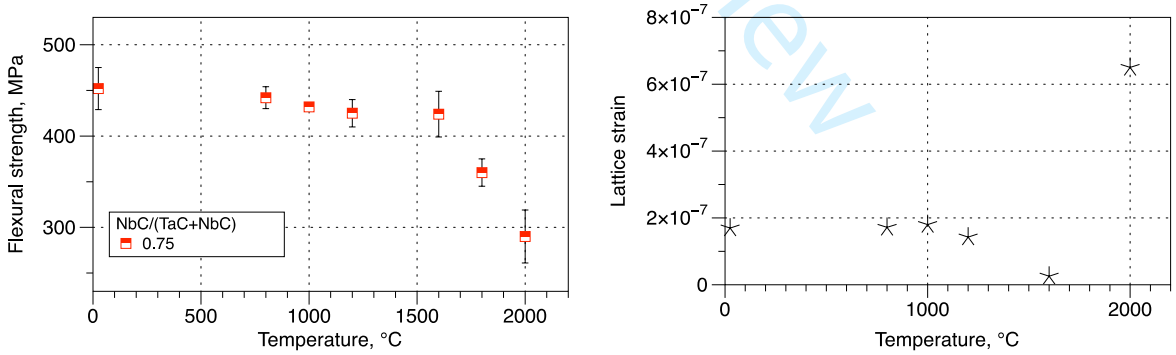

Figure 16. Flexural strength and lattice strain for the 75 mol.% NbC ceramic as a function of the temperature.

As noted before, the relaxation of thermal stresses is one of the factors that may contribute to the strength. For the 75 mol.% NbC ceramic, we evaluated the lattice strain during the Rietveld refinement for the specimens after the high-temperature tests (**Fig. 16 (b)**). We found that for this ceramic, the lattice strain remains constant up to 1200 °C followed by an 85% decrease at 1600 °C. This lattice strain can be attributed to the formation of a solid-solution or directly connected to the cooling after the SPS. The latter seems a more reasonable explanation, as specimens after 2000 °C followed by 20 min cooling to 1570 °C produced a four-fold increase in the lattice strain compared to the cooling during the SPS (2200 °C to 600 °C in 40 min). For this ceramic, the flexural strength remained unchanged up to 1600 °C (**Fig. 16**), suggesting that an additional strengthening mechanism should contribute. Similarly, a ternary solid solution carbide in ref. [21] reported a decrease in strength only above 1600 °C. Such a behavior was connected to the (i) solid solution strengthening and (ii) with a possible shift in the BDTT to the higher temperature range.

As can be seen in **Fig. 14(e)** the fracture at 1600 °C had few grains that fractured in the transgranular manner. Also, the overall porosity of this ceramic was reasonably higher than that for the monolithic TaC or NbC. As mentioned in ref. [40] or [62], the pores may act as a stress relief component, however, the grain size (size and distribution) may also contribute to the increase in the strength in the Hall-Petch like relation. Thus one may consider that some lower number of pores may lead to an

increase in the strength, but the magnitude of such an increase cannot be reasonably high (within or less than 100 MPa).

Creep in the niobium carbide–tantalum carbide system was reported by Kats et al. [12]. It was suggested that the addition of the tantalum carbide within 15– 20 mol.% TaC is the most effective in order to decrease the observed creep rate at 2820 to 3370 K. Based on this study [12], the activation energy for the creep process was 795±62 kJ/mol (190±15 kcal/mol) for all compositions, thus one cannot draw the conclusion if the presence of the solute atoms in the NbC or TaC lattice would have any impact in terms of the atom movement (*see Supl S9* for details on other binary carbide systems). According to Greenwood and Earnshaw [63], the metal and ionic radii for the Nb and Ta atoms are identical; i.e., 146 and 64 pm, respectively. Thus results by Kats et al. [12] support that NbC-rich section of the TaC–NbC system may have higher high-temperature performance. This is consistent with data in **Figs. 12,13**. There may be a cost-saving effect, since tantalum caribe powder is more expensive than for NbC. Depending on the final application, a TaC–NbC solid solution may be preferable to bulk TaC.

Finally, as expected, the total number of experiments performed at 2000 °C may have some effect on the strength. A majority of the data was measured between 200 and 300 MPa. Within this study, the data for the 2000 °C were average for three

specimens. It can be expected that a greater number of tests may provide additional clarification to the reproducibility of the data in **Figure 12** at 2000 °C.

Concluding remarks

Several conclusions can be drawn from the present study. First, it was observed that the lattice parameter and room-temperature strength would have a linear dependence within the studied compositions. This indicates that the lattice parameter for the solid- solutions specimens follows Vegard's law and the formation of the solid solutions leads to an additional increase in strength.

Second, because of the identical thermal processing history, the ceramics had different grain sizes, which may have a separate effect on the high-temperature strength by controlling the grain-boundary sliding. The grain size also contributed to the shape of the temperature dependence of the strength. Among all the studied solid solutions, the 75 mol.% NbC ceramic showed almost an unchanged strength up to 1600 °C (450±20 MPa), following the linear decrease in strength to 290 MPa at 2000 °C. This behavior was correlated with the strain accumulated in the carbide lattice during the SPS process (i.e., solid solution formation and cooling).

Third, the tantalum carbide monolith had a noticeable dependence of the flexural strength on the strain rate at 2000 °C; and, in general, had showed the lowest strength at 2000°C among the studied ceramics.

Finally, the ceramic with 30 mol.% NbC showed that quasi-transgranular fracture can be observed during flexure in the studied temperature range of RT–2000 °C. The overall shape for the cleavage zones depended on the temperature, as a more chaotic orientation of the slip lines was observed below 1200 °C. This finding is most likely connected to a change in the dominant slip-systems as a number of different slip configurations was previously reported for the bulk tantalum and niobium carbides.

Acknowledgements

D.D. was supported by World Premier International Research Center Initiative (WPI), MEXT, Japan.

Compliance with Ethical Standards

The authors declare that they have no conflict of interest.

References

[1] Samsonov GV, Upadhyaya GS, Neshpor VS. Physical Materials Science of Carbides. Kiev, Ukraine: Naukova Dumka; 1974. (In Russian).

[2] Andrievski RA, Spivak II. Strength of Refractory Compounds. Chelyabinsk: Metallurgiya; 1989. (in Russian).

[3] Sheindlin M, Falyakhov T, Petukhov S, Valyano G, Vasin A. Recent advances in the study of high-temperature behaviour of nonstoichiometric TaCx, HfCx and ZrCx carbides in the domain of their congruent melting point. Adv Appl Ceram. 2018;117(sup1):48–55. doi: 10.1080/17436753.2018.1510819

[4] Kelly JP, Graeve OA. Mechanisms of pore formation in high-temperature carbides: Case study of TaC prepared by spark plasma sintering. Acta Mater. 2015;84:472–483. doi: 10.1016/j.actamat.2014.11.005.

[5] Khaleghi E, Lin Y-S, Meyers MA, Olevsky EA. Spark plasma sintering of tantalum carbide. Scr Mater. 2010;63[6]:577–580. doi: 10.1016/j.scriptamat.2010.06.006.

[6] Zhang X, Hilmas GE, Fahrenholtz WG, Deason DM. Hot Pressing of Tantalum Carbide With and Without Sintering Additives. J Am Ceram Soc. 2007;90[2]:393–401. doi: 10.1111/j.1551-2916.2006.01416.x.

[7] Paul A, Binner JGP, Vaidhyanathan B, Heaton ACJ, Brown PM. Oxyacetylene torch testing and microstructural characterization of tantalum carbide. Microscopy 2013;250[2]:122–129. doi: 10.1111/jmi.12028.

[8] Silvestroni L, Pienti L, Guicciardi S, Sciti D. Strength and toughness: the challenging case of TaC-based composites. Composites: Part B. 2015;72:10–20. doi: 10.1016/j.compositesb.2014.11.043.

[9] R. Lowrie, Research on physical and chemical principles affecting high temperature materials for rocket nozzles. Quarterly Progress Report, Contract DA 30-069-ORD-2787. Union Carbide Research Institute, Tarrytown, New York, (1964).

[10] Rudolf CC, Agarwal A, Boels B. TaC–NbC formed by spark plasma sintering with the addition of sintering additives. J Ceram Soc Jpn. 2016;124[4]:381–387. doi: 10.2109/jcersj2.15253.

[11] Sautereau J, Mocellin A. Sintering behaviour of ultrafine NbC and TaC powders. J Mater Sci. 1974;9:761–771. doi: 10.1007/BF00761796.

[12] Kats SM, Ordan'yan SS. Creep in sintered polycrystalline niobium carbide and niobium carbide-based solid solutions. Powder Metall Met Ceram. 1984;23:414–418. doi: 10.1007/BF00796613.

[13] Zubarev PV. High-temperature strength of the interstitial phases. Moscow: Metallurgiya; 1985. (in Russian).

[14] Rafaja D, Lengauer W, Wiesenberger H. Non-metal diffusion coefficients for the Ta–C and Ta–N systems. Acta Mater. 1998;46[10]:3477–3483. doi:10.1016/S1359-6454(98)00036-6.

[15] Rafaja D, Lengauer W, Wiesenberger H, Joguet M. Combined refinement of diffusion coefficients applied on the Nb-C and Nb-N systems. Metall Mater Trans. A 1998;29:439–446. doi: 10.1007/s11661-998-0124-z.

[16] Andrievski RA, Klymentko VV, Khromov YF. Self-diffusion of carbon in transition metal carbides of IV and V group. Phys Met Metallogr. 1969;28[2]:298–303

[17] Matzke H. Diffusion in Carbides and Nitrides. In: Laskar AL, Bocquet JL, Brebec G, Monty C, eds. In: Diffusion in Materials. Dordrecht, Netherlands: Kluwer Academic Publishers, 1990:429–455. doi: 10.1007/978-94-009-1976-1_20.

[18] Fischer JJ. Hot-pressing mixed carbides of Ta, Hf, and Zr. Am Ceram Soc Bull. 1964;43[3]:183–185.

[19] Demirskyi D, Borodianska H, Nishimura T, Suzuki ST, Yoshimi K, Vasylkiv O. Deformation-resistant Ta0.2Hf0.8C solid-solution ceramic with superior flexural strength at 2000°C. J Am Ceram Soc. 2022;105[1]:512–524. doi: 10.1111/jace.18072.

[20] Cedillos-Barraza O, Grasso S, Al Nasiri N, Jayaseelan DD, Reece MJ, Lee WE. Sintering behaviour, solid solution formation and characterisation of TaC, HfC and TaC–HfC fabricated by spark plasma sintering. J Eur Ceram Soc. 2016;36[7]:1539–1548. doi: 10.1016/j.jeurceramsoc.2016.02.009.

[21] Demirskyi D, Borodianska H, Suzuki TS, Sakka Y, Yoshimi K, Vasylkiv O. High-temperature flexural strength performance of ternary high-entropy carbide consolidated via spark plasma sintering of TaC, ZrC and NbC. Scr Mater. 2019;164:12–16. doi: 10.1016/j.scriptamat.2019.01.024.

[22] Demirskyi D, Nishimura T, Suzuki TS, Sakka Y, Vasylkiv O, Yoshimi K. High-temperature toughening in ternary medium-entropy (Ta1/3Ti1/3Zr1/3)C carbide consolidated using spark-plasma sintering. J Asian Ceram Soc. 2020;8[4]:1262–1270. doi: 10.1080/21870764.2020.1840703.

[23] Feng L, Chen W-T, Fahrenholtz WG, Hilmas GE. Strength of single-phase high-entropy carbide ceramics up to 2300°C. J. Am. Ceram. Soc. 2021;104[1]:419–427. doi: 10.1111/jace.17443.

[24] Ivashchenko VI, Turchi PEA, Medukh NR, Shevchenko VI, Gorb L, Leszczynski J. A first-principles study of the stability and mechanical properties of ternary transition metal carbide alloys. J Appl Phys. 2019;125:235101. doi: 10.1063/1.5096646.

[25] Mendelson MI. Average Grain Size in Polycrystalline Ceramics. J Am Ceram Soc. 1969;52[8]:443–448. doi: 10.1111/j.1151-2916.1969.tb11975.x.

[26] Schneider CA, Rasband WS, Eliceiri KW. NIH Image to ImageJ: 25 years of image analysis. Nature Methods 2012;9[7]:671–675. doi:10.1038/nmeth.2089.

[27] Demirskyi D, Vasylkiv O. Analysis of the high-temperature flexural strength behavior of B4C–TaB2 eutectic composites produced by in situ spark plasma sintering. Mater Sci Eng A. 2017;697:71–78. doi: 10.1016/j.msea.2017.04.093.

[28] Demirskyi D, Vaslykiv O. Spark plasma sintering and high-temperature strength of B6O–TaB2 ceramics. J Eur Ceram Soc. 2017;37[8]:3009–3014. doi: 10.1016/j.jeurceramsoc.2017.02.052.

[29] Norton JT, Mowry AL. Solubility relationships of the refractory monocarbides. JOM 1949;1:133–136. doi: 10.1007/BF03398086.

[30] Wells M, Pickus M, Kennedy K, Zackay V. Superconductivity of Solid Solutions of TaC and NbC. Phys Rev Lett. 1964;12:536. doi: 10.1103/PhysRevLett.12.536.

[31] Bowman AL. The variation of lattice parameter with carbon content of tantalum carbide. J Phys Chem. 1961;65[9]:1596–1598. doi: 10.1021/j100905a028.

[32] Storms EK, Krikorian NH. The Variation of Lattice Parameter with Carbon Content of Niobium Carbide. J Phys Chem. 1959;63[10]:1747–1749. doi: 10.1021/j150580a042.

[33] Holleck H. Material selection for hard coatings. J Vac Sci Technol A. 1986;4[6]:2661–2669. doi: 10.1116/1.573700.

[34] Lengauer W. Transition metal carbides, nitrides and carbonitrides. In: Riedel R, eds. Chapter 7 in Handbook of Ceramic Hard Materials. Weinheim: Wiley-VCH Verlag; 2008:202–252. doi: 10.1002/9783527618217.ch7.

[35] Gridneva IV, Mil'man YuV, Synel'nikova VS, Chugunova SI. Influence of temperature on the mechanism of failure and mechanical properties of niobium carbide single crystals. Phys. Met. 1982;4[5];74–79. (In Russian).

[36] Grigor'ev ON, Trefilov VI, Shatokhin AM. Influence of temperature on the failure of brittle materials in concentrated loading. Sov Powder Metall Met Ceram. 1983;22:1028–1033. doi: 10.1007/BF00802434.

[37] Hackett K, Verhoef S, Cutler RA, Shetty DK. Phase Constitution and Mechanical Properties of Carbides in the Ta–C System. J Am Ceram Soc. 2009;92[10]:2404–2407. doi: 10.1111/j.1551-2916.2009.03201.x.

[38] Woydt M, Mohrbacher H, Vleugels J, Huang S. Tailoring the functional properties of niobium carbide. In: Ohji T, Halbig M, Moon KI, Singh M, eds. Advanced Processing and Manufacturing Technologies for Nanostructured and Multifunctional Materials III. Ceram Eng Sci Proc. 2017;37[5]:101–113. doi: 10.1002/9781119321736.ch11. (2017)

[39] Anstis GR, Chantikul P, Lawn BR, Marshall DB. A critical evaluation of 1ndentation techniques for measuring fracture toughness: I, direct crack measurements. J Am Ceram Soc. 1981;64[9]:533–538. doi: 10.1111/j.1151-2916.1981.tb10320.x.

[40] Demirskyi D, Nishimura T, Sakka Y, Vasylkiv O. High-strength TiB2–TaC ceramic composites prepared using reactive spark plasma consolidation. Ceram Int. 2016;42:1298–1306. doi: 10.1016/j.ceramint.2015.09.065.

[41] Hollox GE. Microstructure and mechanical behavior of carbides. Mater Sci Eng. 1968;3[3]:121–137. Doi: 10.1016/0025-5416(68)90001-3.

[42] Johansen HA, Cleary JG. The ductile-brittle transition in tantalum carbide. J Electrochem Soc. 1966;113[4]:378–381. doi: 10.1149/1.2423967.

[43] Kosolapova TYa. Properties, Synthesis and Application of Refractory Compounds. Reference Book, Moscow: Metallurgiya; 1986. (In Russian).

[44] Hoffman M, Williams WS. A simple model for the deformation behaviour of tantalum carbide. J Am Ceram Soc. 1986;69[8]:612–614. doi: 10.1111/j.1151-2916.1986.tb04817.x.

[45] Samsonov GV, Upadhyaya GS, Neshpor VS. Physical Materials Science of Carbides, Kiev, Ukraine: Naukova Dumka; 1974. (In Russian).

[46] Demirskyi D, Vasylkiv O, Yoshimi K. High-temperature deformation in bulk polycrystalline hafnium carbide consolidated using spark plasma sintering. J Eur Ceram Soc. 2021;41[15]:7442–7449. doi: 10.1016/j.jeurceramsoc.2021.08.038.

[47] Ordan'yan SS, Stepanenko EK, Sokolov IV. Strength of NbC-NbB2 sintered composites. Izv. Vyssh. Uchebn. Zaved., Khim. Khim T. 1984;27[10]:1201–1203. (In Russian).

[48] Kelly A, Rowcliffe DJ. Deformation of Poly crystalline Transition Metal Carbides. J Am Ceram Soc. 1967;50[5]:253–256. doi: 10.1111/j.1151-2916.1967.tb15098.x.

[49] Demirskyi D, Suzuki TS, Yoshimi K, Vasylkiv O. Synthesis and high-temperature properties of medium-entropy (Ti,Ta,Zr,Nb)C using the spark plasma consolidation of carbide powders. Open Ceramics. 2020;2:100015. doi: 10.1016/j.oceram.2020.100015.

[50] Lanin AG, Zubarev PV, Vlasov KP. Mechanical and thermophysical properties of materials in HTGR fuel bundles. At. Energy. 1993;74(1):40–44. doi: 10.1007/BF00750973.

[51] Sanders WA, Probst HB. High-temperature mechanical properties of polycrystalline hafnium carbide and hafnium carbide containing 13 vol.% hafnium diboride. Report NASA-TN-D-5008. NASA Lewis Research Centre, Cleveland, Ohio, 1963.

[52] Mohanty GP, Fiegel LJ, Healy JH. Unit cell and space group of 2Nb2O5.Ta5O5. Acta Cryst. 1962;15:1190. doi: 10.1107/S0365110X62003151.

[53] Holtzberg F, Reisman A. Sub-solidus equilibria in the system Nb2O5-Ta2O5[1]. J Phys Chem. 1961;65[7]:1192–1196. doi: 10.1021/j100825a024.

[54] Hidde J, Guguschev C, Klimm D. Thermal analysis and crystal growth of doped Nb2O5. J. Cryst. Growth. 2019;509:60–65. doi: 10.1016/j.jcrysgro.2018.12.035.

[55] Liu J-X, Kan Y-M, Zhang G-J. Pressureless Sintering of Tantalum Carbide Ceramics without Additives. J Am Ceram Soc. 2010;93[2]:370–373. doi: 10.1111/j.1551-2916.2009.03437.x.

[56] Hannink RHJ, Kohlstedt DL, Murray MJ. Slip System Determination in Cubic Carbides by Hardness Anisotropy. Proc. R. Soc. Lond. A . 1972;326:409–420. doi: http://www.jstor.org/stable/78013.

[57] Lee DW, Haggerty JS. Plasticity and Creep in Single Crystals of Zirconium Carbide. J Am Ceram Soc. 1969;52[12]:641–647. doi: 10.1111/j.1151-2916.1969.tb16067.x.

[58] Kelly A, Rowcliffe DJ. Slip in Titanium Carbide. Phys Stat Sol. 1966;14[1]:K29–K33. Doi: 10.1002/pssb.19660140132.

[59] Smith CJ, Ross MA, De Leon N, Weinberger CR, Thompson GB. Ultra-high temperature deformation in TaC and HfC. J Eur Ceram Soc. 2018;38 [16]:5319–5332. doi: 10.1016/j.jeurceramsoc.2018.07.017.

[60] Rowcliffe DJ, Hollox GE. Plastic flow and fracture of tantalum carbide and hafnium carbide at low temperatures. J Mater Sci. 1971;6[10]:1261–1269. doi: 10.1007/BF00552039.

[61] Rowcliffe DJ, Hollox GE. Hardness anisotropy, deformation mechanisms and brittle-to-ductile transition in carbide. J Mater Sci. 1971;6[10]:1270–1276. doi: 10.1007/BF00552040.

[62] Johari O, Parikh NM. Scanning Electron Fractographic Study of Aluminum Oxide as a Function of Testing Temperature and Grain Size. In: Bradt RC, Hasselman DPH, Lange FF, eds. In: Concepts, Flaws, and Fractography. Fracture Mechanics of Ceramics. vol 1. Boston, MA: Springer, 1974:399–420. doi: 10.1007/978-1-4684-2991-6_21.

[63] Greenwood NN, Earnshaw A. Chemistry of the Elements. 2nd edition. Oxford: Butterworth-Heinemann; 1998.

Tables

Table 1 Composition of the powder mixtures used consolidation by the SPS method

Composition ID	NbC/(NbC+TaC), a.u.	NbC, mol.%
0NC	0	0
03NC	0.3	30
05NC	0.5	50
06NC	0.66	66
07NC	0.75	75
1NC	1.0	100

Table 2 Physical and mechanical properties of bulks in the TaC–NbC system

ID	Lattice parameter, Å	Theoretical density, g/cm^3	Bulk density, g/cm^3	Median grain size^X, μm	Hardness, GPa^Y	Toughness^Z, MPa m$^{1/2}$	Room temperature strength, MPa
0NC	4.445(2)	14.58	14.474	31.2±20.5	14.6	3.1	580±18
03NC	4.452(5)	12.52	11.985	21.9±11.0	14.7	4.7	624±23
05NC	4.457(8)	11.15	11.010	17.3±7.9	15.2	4.0	480±20
06NC	4.462(0)	10.07	9.745	18.1±10.0	15.8	3.7	483±12
07NC	4.464(2)	9.46	9.326	19.2±12.0	15.7	3.2	452±17
1NC	4.467(5)	7.80	7.626	16.4±6.9	15.5	3.4	440±26

X – error is the standard deviation;
Y – 98 N tests, error in hardness did not exceed ±0.8 GPa;
Z – error is within ±0.2 MPa m$^{1/2}$.

Figure captions

Figure 1. Shrinkage behavior of the powder compacts at the heating rate of 500 °C/min and the constant pressure of 34 kN.

Figure 2. The lattice constant of the solid-solution carbides in the TaC–NbC system as a function of the NbC content [12,29,30]. (b) shows the refinement of the equimolar ceramic using the lattice parameter of 4.457(8) Å. (c) shows peak shift for all compositions in the TaC–NbC system.

Figure 3. The lattice constant of the TaC and NbC as a function of the C to metal ratio [31, 32]. Dash line is for the lattice parameter of TaC and NbC bulks after the SPS consolidation.

Figure 4. Representative microstructure of ceramics in the TaC–NbC system after SPS: a) 0NC b) 03NC, c) 05NC, d) 06NC, e) 07NC, and f) 1NC.

Figure 5. Hardness in the TaC–NbC as a function of the NbC content and hardness data according to the first-principles calculations in ref. [24]. Dashed lines indicate the 95% confidence intervals for the regression line.

Figure 6. Relation between hardness and fracture toughness in the TaC–NbC system, and for TaC [6,8,20,33,34] and NbC [33–38] bulks. The toughness in [8] was measured by the flexure approach. Horizontal dot lines are for the hardness. Vertical dashed line and shaded area are for the toughness determined in [8] and [35] for TaC and NbC, respectively.

Figure 7. Temperature dependence of the flexural strength of bulk TaC [7,40–43].

Figure 8. Effect of temperature of the flexural test on the fracture behavior of the monolithic tantalum carbide. (a,b) 800 °C; (c,d) 1600°C, and (e,f) 2000 °C.

Figure 9. Temperature dependence of mechanical properties of niobium carbide ceramics [2,35,43,47,48]. (a) flexural strength and (b) hardness and toughness for bulk NbC by Grigor'ev et al. [36]. Vertical dash line corresponds to the sharpest maximum in the length of the radial crack observed during the indentation process in ref. [36]. Data from ref. [2] are for annealed and as-consolidated specimens.

Figure 10. Representative fracture of ceramics in the TaC–NbC system during the flexural strength tests at 2000 °C. a) 0NC, b) 03NC, c) 05NC, d) 06NC, e) 07NC, and f) 1NC.

Figure 11. Representative fracture of ceramics in the TaC–NbC system during the flexural strength tests at RT and 800 °C. a) 0NC, b) 03NC, c) 05NC, d) 06NC, e) 07NC, and f) 1NC. a,b,f 800 °C and c,d,e RT.

Figure 12. Flexural strength in the TaC–NbC system as a function of the testing temperature and NbC content.

Figure 13. Flexural strength as a function of the homologous temperature and NbC content.

Figure 14. Representative fracture of ceramics in the TaC–NbC system during the flexure at 1600 °C. a) 0NC b) 03NC, c) 05NC, d) 06NC, e) 07NC, and f) 1NC.

Figure 15. Effect of temperature of the flexural test on the fracture of the 03NC ceramic at (a) 800 °C, (b) 1000 °C, (c) 1200 °C, (d) 1600 °C, (e)1800 °C, and (f) at 2000 °C.

Figure 16. Flexural strength and lattice strain for the 75 mol.% NbC ceramic as a function of the temperature.

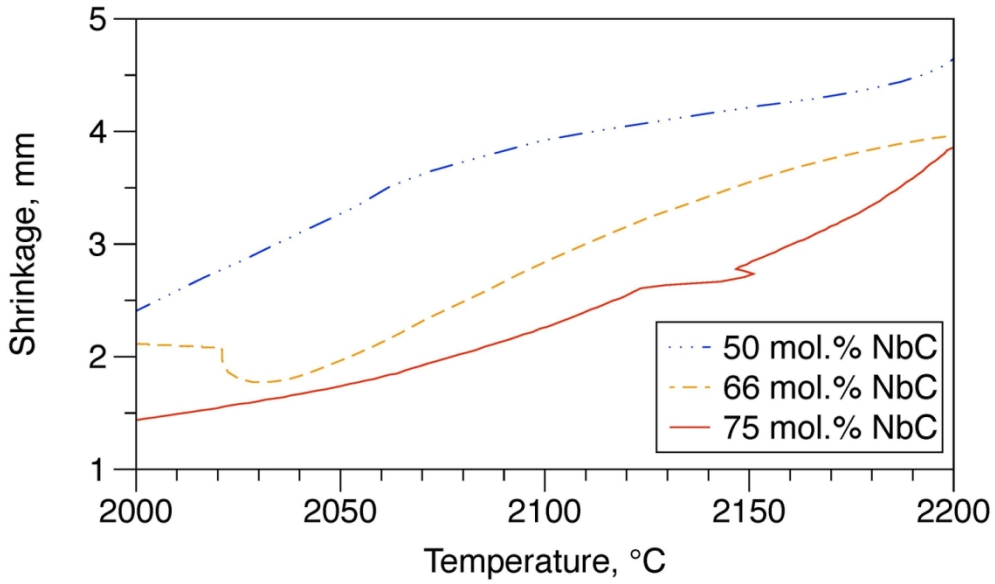

Figure 1. Shrinkage behavior of the powder compacts at the heating rate of 500 °C/min and the constant pressure of 34 kN.

127x76mm (300 x 300 DPI)

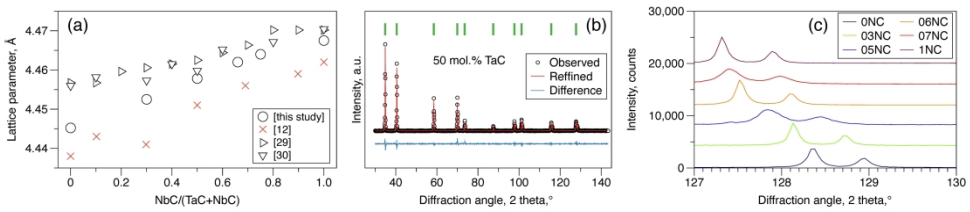

Figure 2. The lattice constant of the solid-solution carbides in the TaC–NbC system as a function of the NbC content [12,29,30]. (b) shows the refinement of the equimolar ceramic using the lattice parameter of 4.457(8) Å. (c) shows peak shift for all compositions in the TaC–NbC system.

363x76mm (300 x 300 DPI)

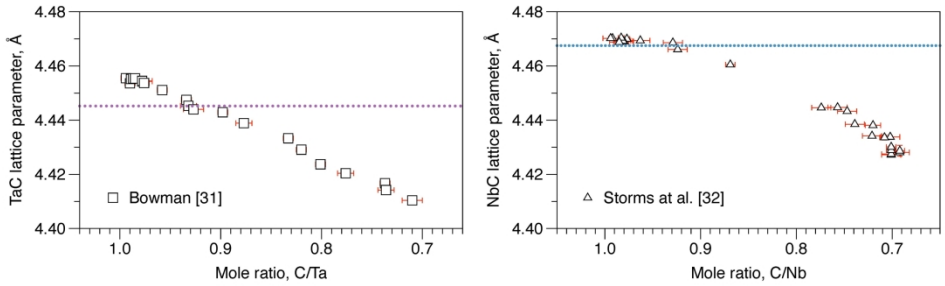

Figure 3. The lattice constant of the TaC and NbC as a function of the C to metal ratio [31, 32]. Dash line is for the lattice parameter of TaC and NbC bulks after the SPS consolidation.

264x76mm (300 x 300 DPI)

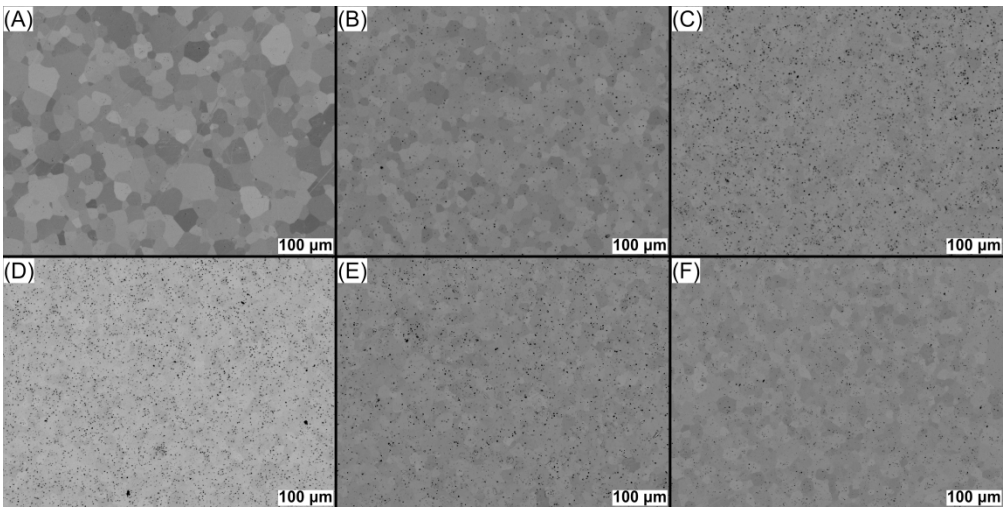

Figure 4. Representative microstructure of ceramics in the TaC–NbC system after SPS: a) 0NC b) 03NC, c) 05NC, d) 06NC, e) 07NC, and f) 1NC.

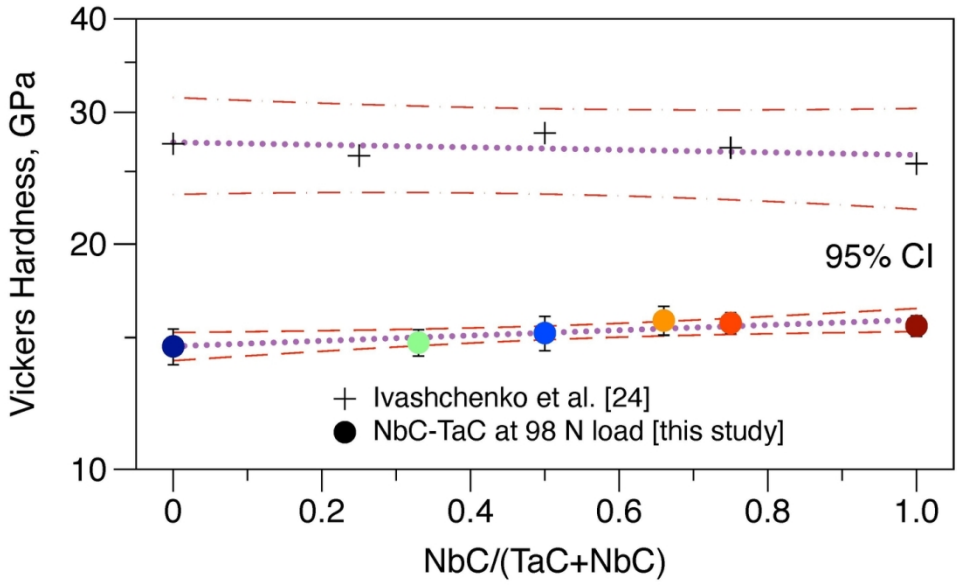

Figure 5. Hardness in the TaC–NbC as a function of the NbC content and hardness data according to the first-principles calculations in ref. [24]. Dashed lines indicate the 95% confidence intervals for the regression line.

127x76mm (300 x 300 DPI)

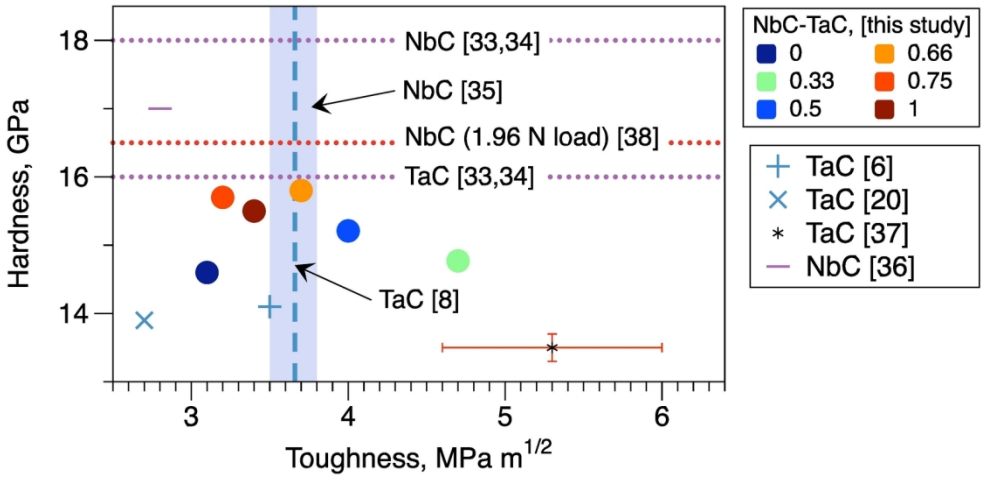

Figure 6. Relation between hardness and fracture toughness in the TaC–NbC system, and for TaC [6,8,20,33,34] and NbC [33–38] bulks. The toughness in [8] was measured by the flexure approach. Horizontal dot lines are for the hardness. Vertical dashed line and shaded area are for the toughness determined in [8] and [35] for TaC and NbC, respectively.

152x76mm (300 x 300 DPI)

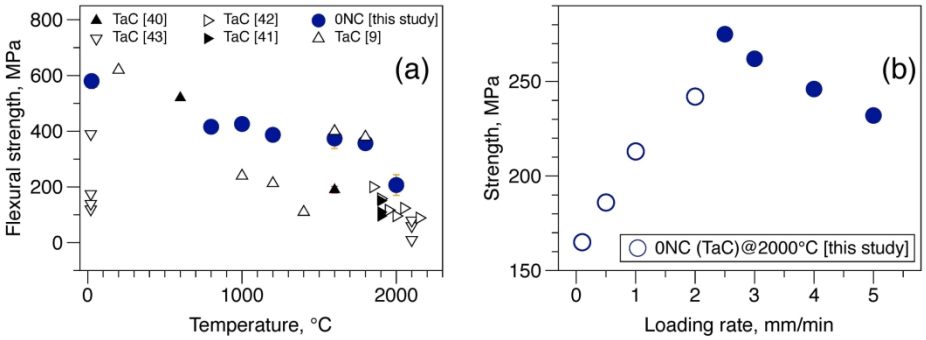

Figure 7. Temperature dependence of the flexural strength of bulk TaC [7,40–43].

215x76mm (300 x 300 DPI)

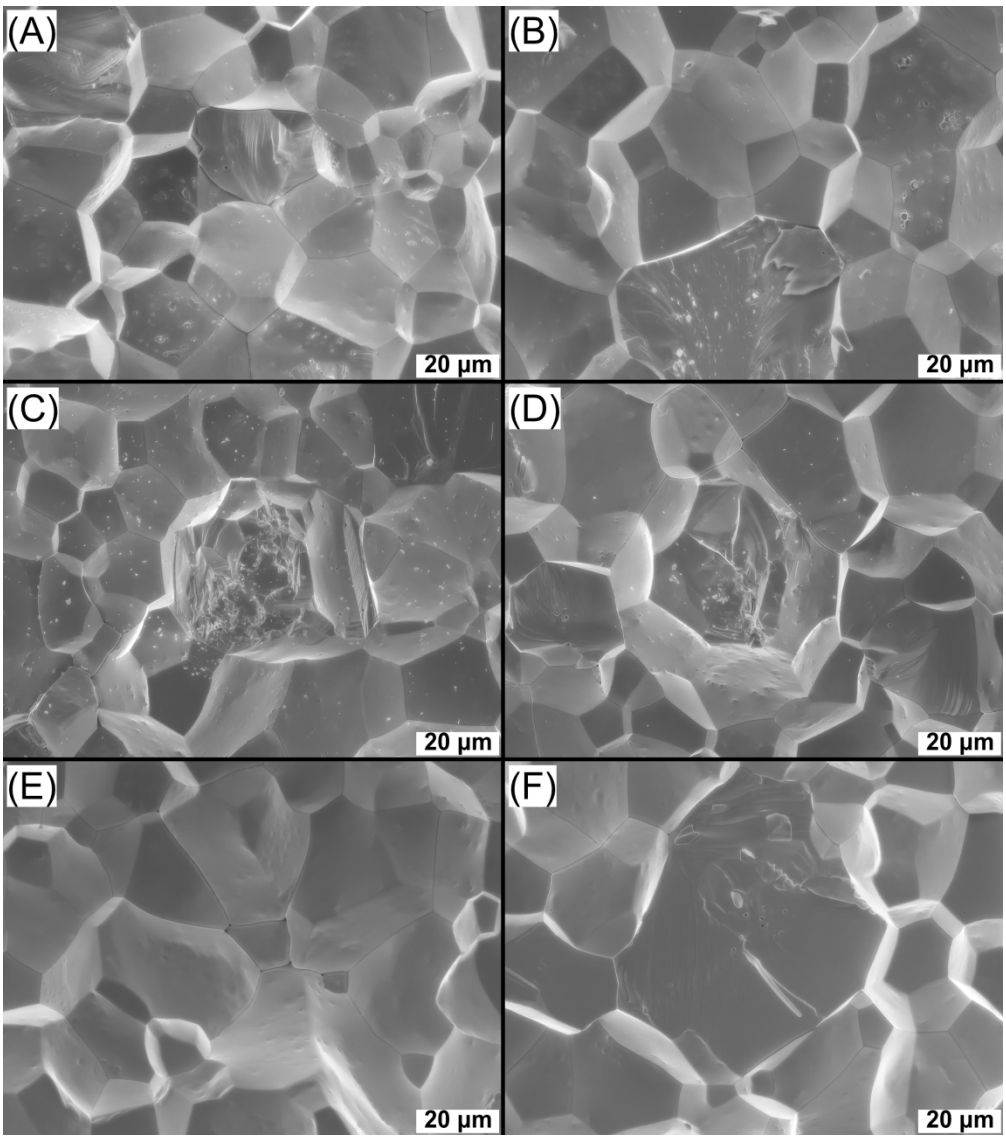

Figure 8. Effect of temperature of the flexural test on the fracture behavior of the monolithic tantalum carbide. (a,b) 800 °C; (c,d) 1600°C, and (e,f) 2000 °C.

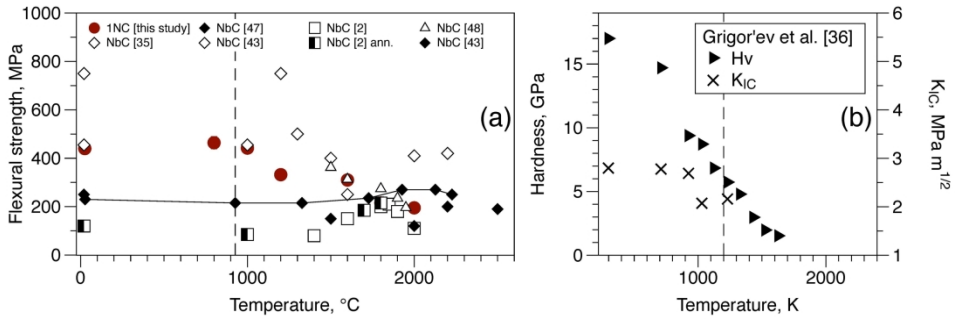

Figure 9. Temperature dependence of mechanical properties of niobium carbide ceramics [2,35,43,47,48]. (a) flexural strength and (b) hardness and toughness for bulk NbC by Grigor'ev et al. [36]. Vertical dash line corresponds to the sharpest maximum in the length of the radial crack observed during the indentation process in ref. [36]. Data from ref. [2] are for annealed and as-consolidated specimens.

236x78mm (300 x 300 DPI)

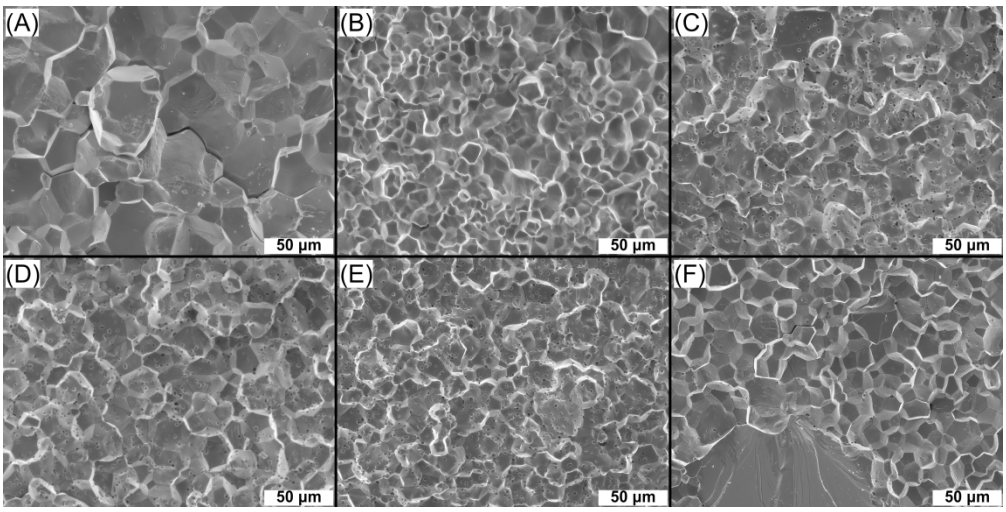

Figure 10. Representative fracture of ceramics in the TaC–NbC system during the flexural strength tests at 2000 °C. a) 0NC, b) 03NC, c) 05NC, d) 06NC, e) 07NC, and f) 1NC.

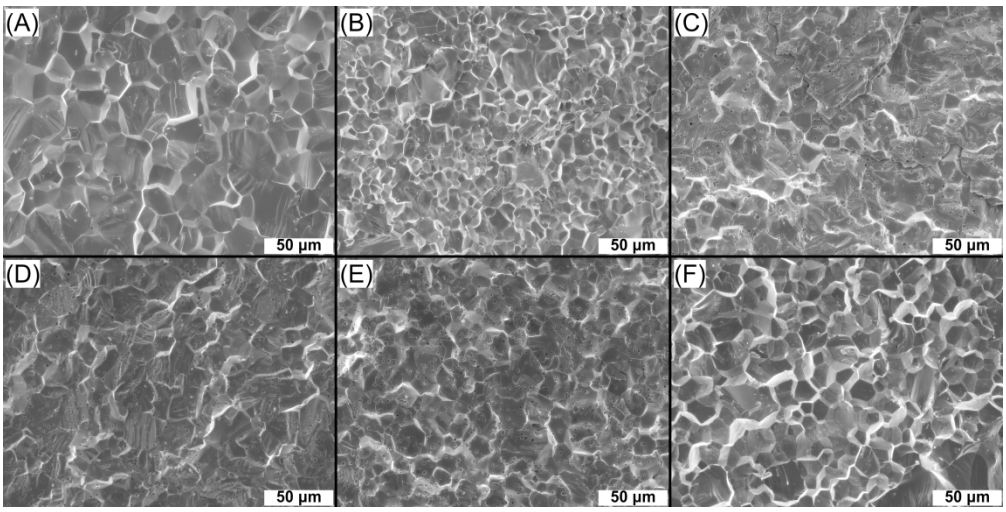

Figure 11. Representative fracture of ceramics in the TaC–NbC system during the flexural strength tests at RT and 800 °C. a) 0NC, b) 03NC, c) 05NC, d) 06NC, e) 07NC, and f) 1NC. a,b,f 800 °C and c,d,e RT.

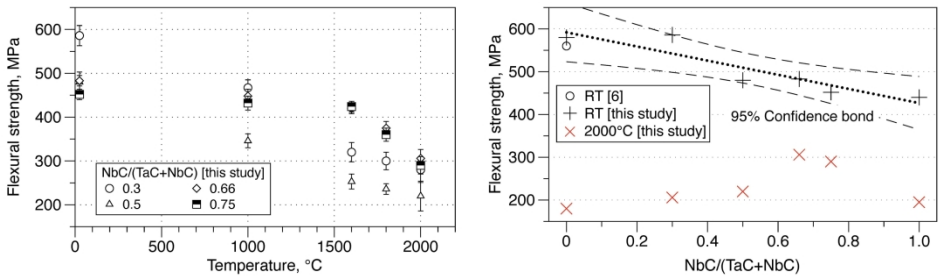

Figure 12. Flexural strength in the TaC–NbC system as a function of the testing temperature and NbC content.

266x81mm (300 x 300 DPI)

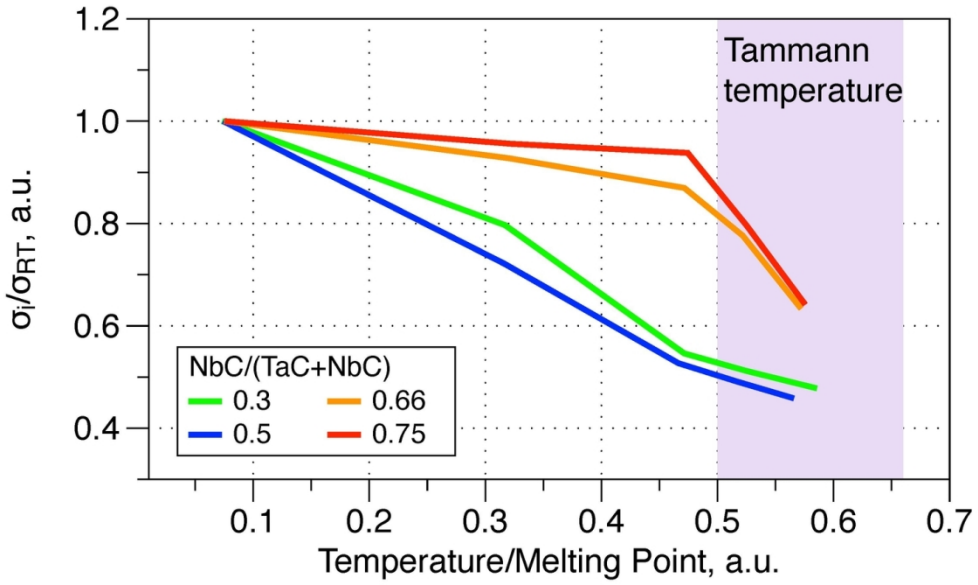

Figure 13. Flexural strength as a function of the homologous temperature and NbC content.

127x76mm (300 x 300 DPI)

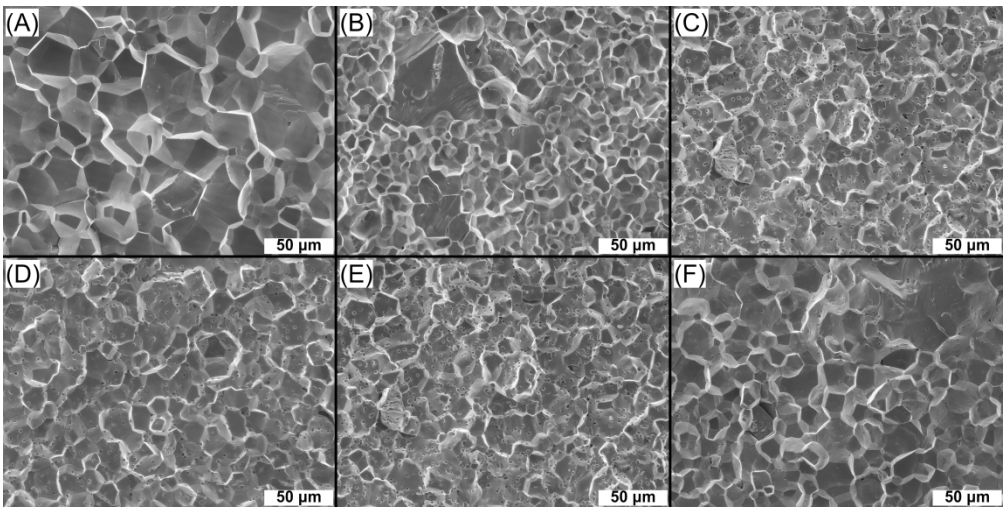

Figure 14. Representative fracture of ceramics in the TaC–NbC system during the flexure at 1600 °C. a) 0NC b) 03NC, c) 05NC, d) 06NC, e) 07NC, and f) 1NC.

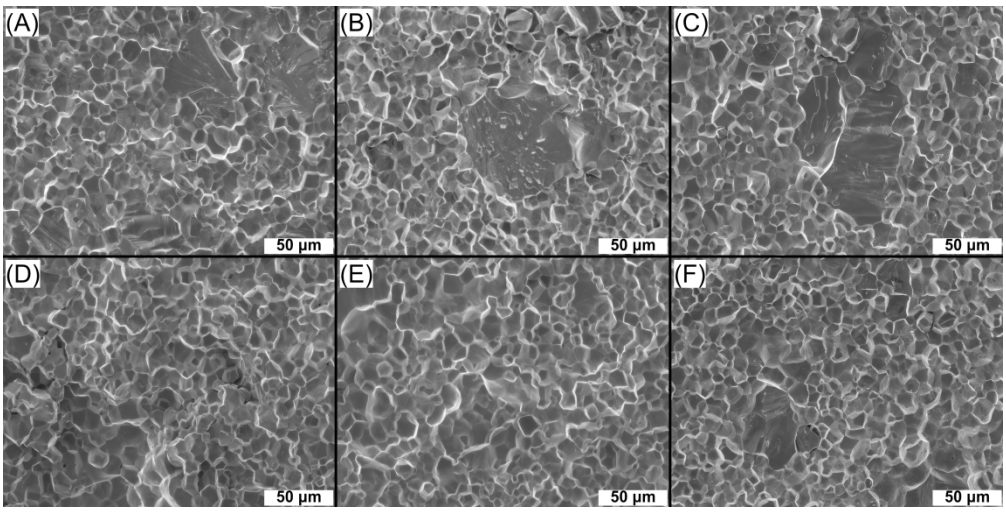

Figure 15. Effect of temperature of the flexural test on the fracture of the 03NC ceramic at (a) 800 °C, (b) 1000 °C, (c) 1200 °C, (d) 1600 °C, (e)1800 °C, and (f) at 2000 °C.

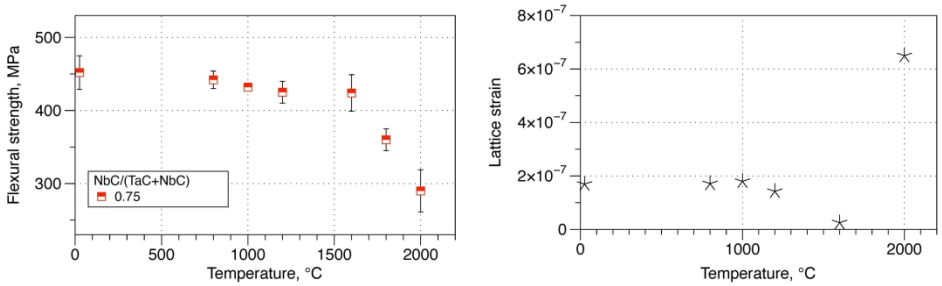

Figure 16. Flexural strength and lattice strain for the 75 mol.% NbC ceramic as a function of the temperature.

266x81mm (300 x 300 DPI)

Supporting Information

Consolidation and high-temperature properties of ceramics in the TaC–NbC system

D. Demirskyi †, T. Nishimura, T.S. Suzuki, K. Yoshimi, O. Vasylkiv†.

E-mail: demirskyi.dmytro.e2@tohoku.ac.jp, oleg.vasylkiv@nims.go.jp.

Appendix

Supporting information, *S1. Diffusion in the TaC–NbC system*

Lanin [R1] reported diffusion of metal and carbon in selected carbides at various temperatures (**Fig. S1**). It is clear here that diffusion in solid-solutions should be faster than in monolithic carbides.

Diffusion of carbon in NbC and TaC was studied by Andrievski et al. [R2]. Rafaja et al. [R3,R4] and These studies were performed at different temperatures. However, results indicate that carbon will diffuse in NbC faster that in TaC (**Fig. S2**).

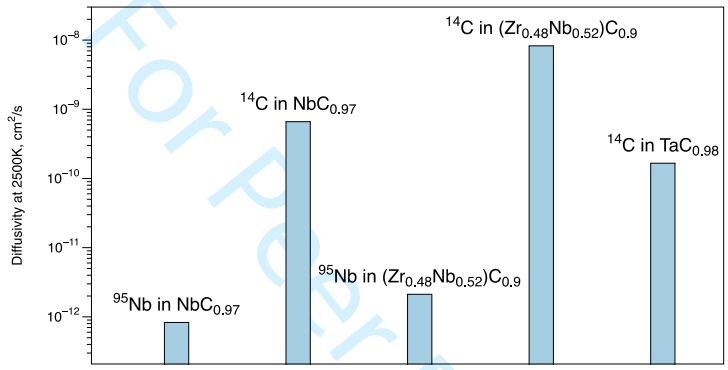

Figure S1. Diffusivity in various carbides at 2500K [R1].

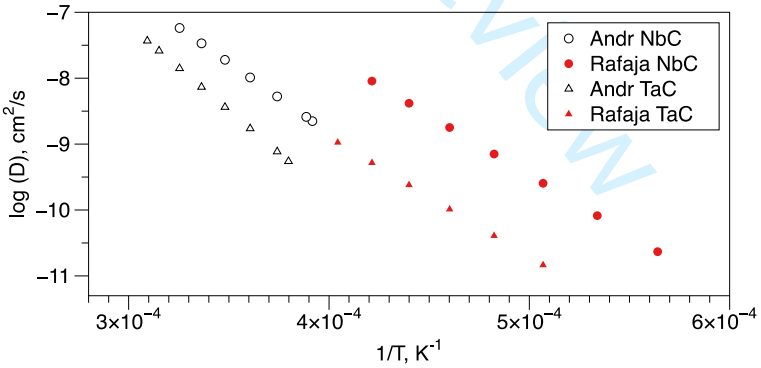

Figure S2. Diffusivity in TaC and NbC according to [R2–R4].

P-3

Supporting information, S2. *Initial powders*

Initial powders were TaC (Lot #LKP4101) and NbC (Lot #W19E52) by Wako Pure Chemical Industries. The particle size of tantalum carbide was finer than 2 μm, while the NbC had median size of below 5 μm. However, for NbC one can observe large particles with size up to 20 μm (**Figure S3**)

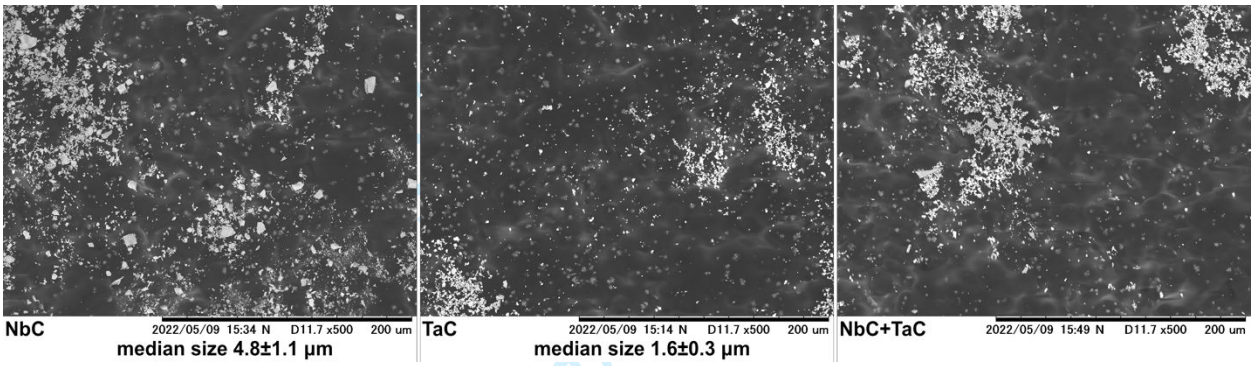

Figure S3. SEM images of the initial powders used for the SPS processing.

Supporting information, *S3. Grain size for SPSed ceramics in the TaC–NbC system*

Grain size was analyzed using a custom MatLab (The MathWorks, Inc., Natick, MA, US) code which calculated the grain size using an intercept technique. The grain boundaries are detected automatically with a nice level of accuracy using a self-learning algorithm. **Figures S4** to **S9** provide a summary for grain size determined by this approach.

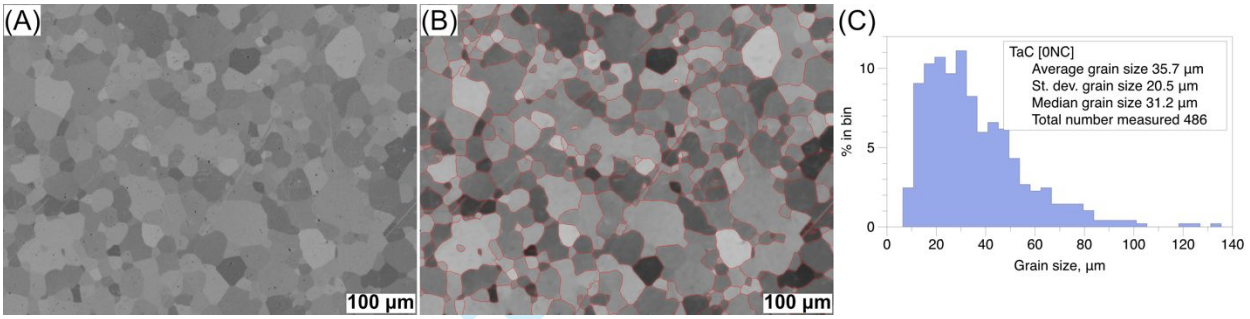

Figure S4. Representative image of polished TaC ceramic. (b) shows the grain boundaries evaluated by a self-learning engine. (c) summarizes average and median size that were quantitatively measured by an intercept technique.

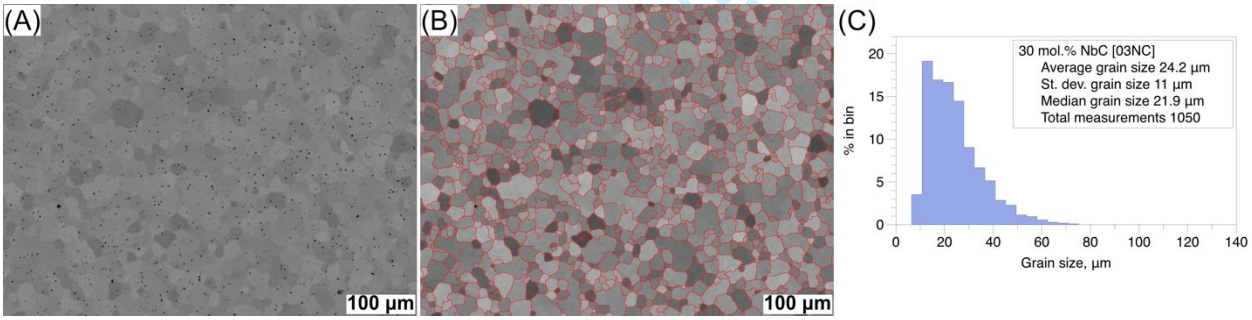

Figure S5. Representative image of polished 30 mol.% NbC (03NC) ceramic. (b) shows the grain boundaries evaluated by a self-learning engine. (c) summarizes average and median size that were quantitatively measured by an intercept technique.

P-5

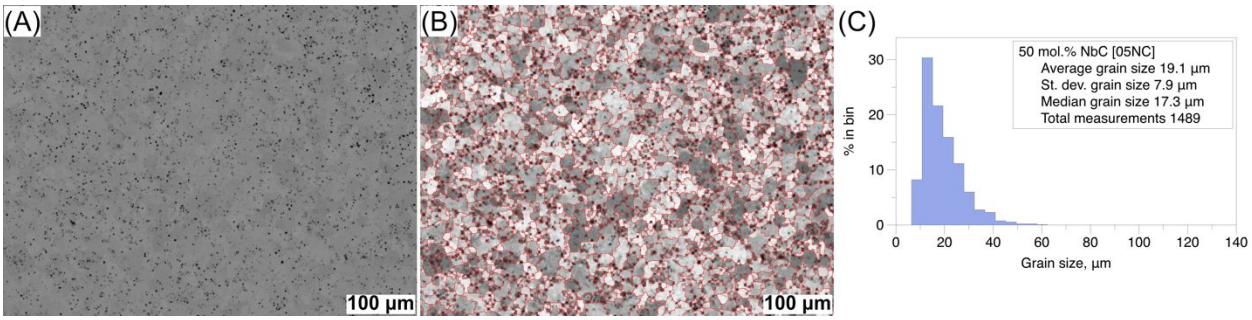

Figure S6. Representative image of polished 50 mol.% NbC (05NC) ceramic. (b) shows the grain boundaries evaluated by a self-learning engine. (c) summarizes average and median size that were quantitatively measured by an intercept technique.

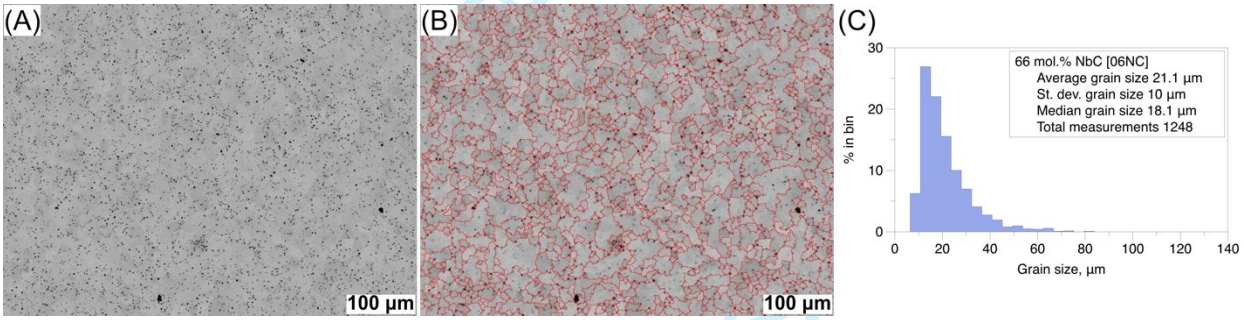

Figure S7. Representative image of polished 66 mol.% NbC (06NC) ceramic. (b) shows the grain boundaries evaluated by a self-learning engine. (c) summarizes average and median size that were quantitatively measured by an intercept technique.

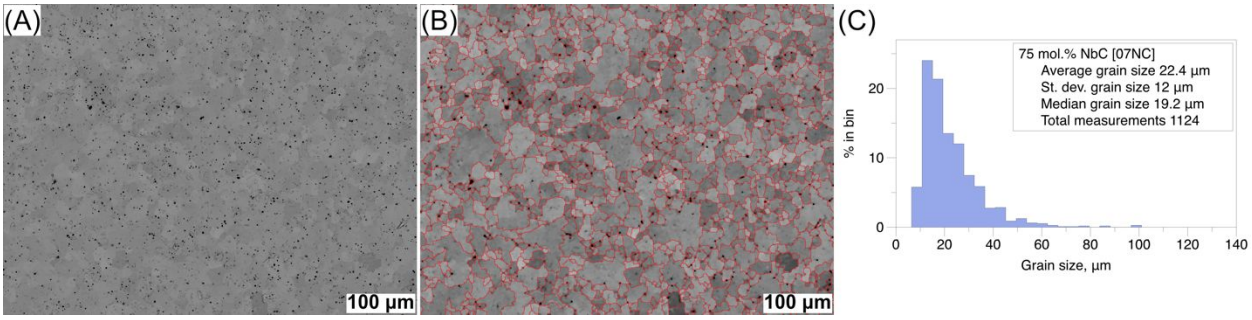

Figure S8. Representative image of polished 75 mol.% NbC (07NC) ceramic. (b) shows the grain boundaries evaluated by a self-learning engine. (c) summarizes average and median size that were quantitatively measured by an intercept technique.

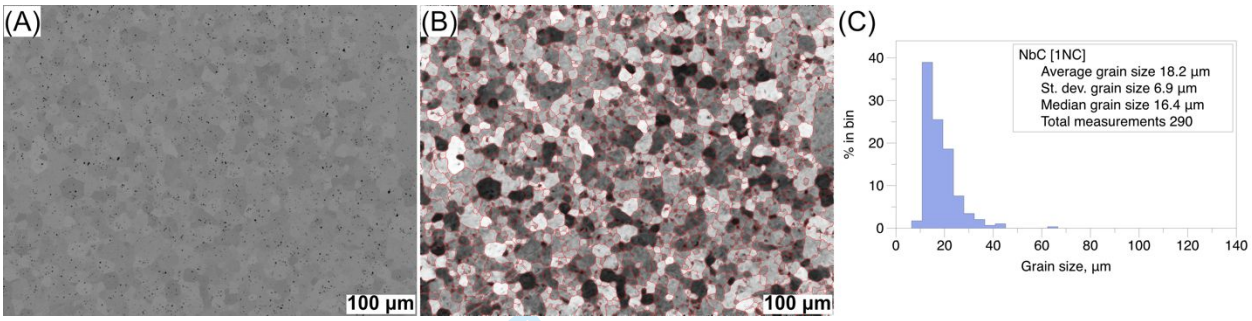

Figure S9. Representative image of polished NbC ceramic. (b) shows the grain boundaries evaluated by a self-learning engine. (c) summarizes average and median size that were quantitatively measured by an intercept technique.

Supporting information, *S4. Porosity for SPSed ceramics in the TaC–NbC system*

To estimate the overall level of porosity, the SEM image was analyzed using Fiji software. A threshold was applied so that the dark regions (pores) were highlighted. The area of the pores was calculated by the software. The porosity % was calculated by the equation given: Porosity % = 100 (Area of pores / Total area). An example is illustrated in **Figure S10**, while results are summarized in **Table T1**.

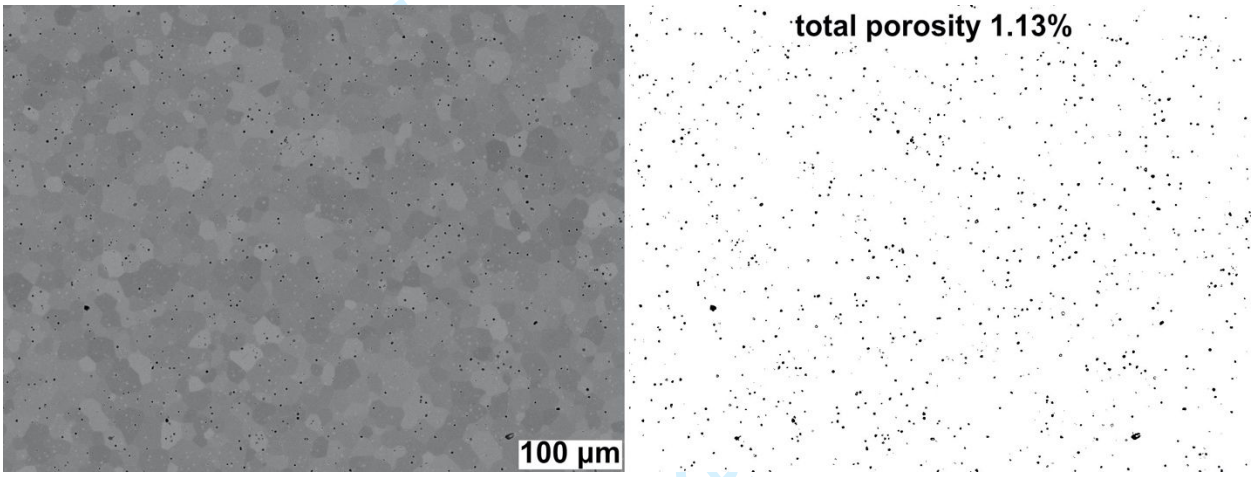

Figure S10. Example porosity calculation.

Table T1 Density and porosity of bulks in the TaC–NbC system

ID	Theoretical density, g/cm^3	Bulk density, g/cm^3	Porosity based on density, %	Porosity based on SEM, % average	median
0NC	14.58	14.474	0.72	0.05	0.08
03NC	12.52	11.985	4.27	2.28	2.46
05NC	11.15	11.010	1.25	1.92	2.11
06NC	10.07	9.745	3.22	2.32	3.25
07NC	9.46	9.326	1.41	0.63	0.69
1NC	7.80	7.626	2.23	0.40	0.51

Supporting information, *S5. Calculation of stress exponents during the SPS*

The shrinkage data during sintering process can be used to identify the dominant consolidation mechanism. For this reason we used the model proposed by Bernard-Granger and Guizard [R5] for their analysis. This model is based on the creep deformation process of bulk ceramics which should satisfy the following equation 1

$$\dot{\varepsilon} = \frac{d\varepsilon}{dt} = A\frac{DG_0\boldsymbol{b}}{kT}\left(\frac{\boldsymbol{b}}{d}\right)^p\left(\frac{\sigma_{macro}}{G_0}\right)^n (1)$$

where, $\dot{\varepsilon}$ is creep rate, A – constant, D – diffusion coefficient, G_0 – shear modulus, $\boldsymbol{b}$ – the Burgers vector, k – Boltzmann's constant, T – absolute temperature, d – grain size, σ_{macro} macroscopic applied stress, p – inverse grain size exponent, and n is stress exponent, while t is time.

Using a fixed densification rate of (i.e., 1×10^{-4} s^{-1}) one can analyze the stress exponent n in the eq. 1. Within this study we also applied this approach, while the key parameters for the (eq.1) were green density 60% of TD, G_0 = 189 GPa for NbC and G_0 = 215 GPa for TaC [R6], Poisson's ratio 0.23 and σ_{macro}= 48 MPa (38 kN for the 30-mm die). The G_0 for the solid solution were calculated using a rule of mixtures.

The effective pressure (σ_{eff}) and shear modulus (G_{eff}) are calculated using the following relations [R7] and from the variation of relative density with time as shown in Figure 1b in the main manuscript.

$$\sigma_{eff} = \frac{(1-\rho_0)}{\rho^2(\rho-\rho_0)}\times\sigma_{macro}$$

$$G_{eff} = \frac{G_0(1-P)}{(1+BP)} \qquad B = 11-19\frac{\nu}{4(1+\nu)}$$

The term $\ln\left[(1/G_{eff})(1/\rho)(d\rho/dt)\right]$ is plotted against $\ln(\sigma_{eff}/G_{eff})$. The slope of the linear fit gives the stress exponent, n. For this purpose we composed the MatLab

(The MathWorks, Inc., Natick, MA, US) code for analysis of the SPS shrinkage. The typical output is presented in **Figure S11**. For a fixed densification rate such as 1×10^{-3} s^{-1} one can calculate the *n*. **Figure S12** shows the results for the niobium carbide (1NC). The observed and calculated parameters are tabulated in **Table T2**. The *n* value is less than 2, which signifies the dominance of diffusion mechanism during densification. The values of *n* greater than 2 (but less than 5) dislocation based activities during deformation/densification. Generally, contribution of diffusion should increase at high temperatures. Thus the values of stress exponents were expected to be < 2 at higher sintering temperature. The *n* value of 2 should correspond to the grain-boundary sliding mechanism, or, perhaps, grain-boundary diffusion in this case, while *n*~1 indicates diffusion based mechanism is active. Considering data for other temperatures, we evaluated *n* for the bulk NbC at 2000 °C and 2100 °C and found that the n value decreases from 2. This suggests that for a given densification rate there are several mechanisms that are active. Evaluation of the activation energy for this short temperature window, and assuming $n = 2$, would yield the value of 352±18 kJ/mol. Lanin [R1] reported that the activation energy for the diffusion ^{95}Nb and ^{14}C niobium carbide is 530 kJ/mol and 420 kJ/mol, respectively.

P-10

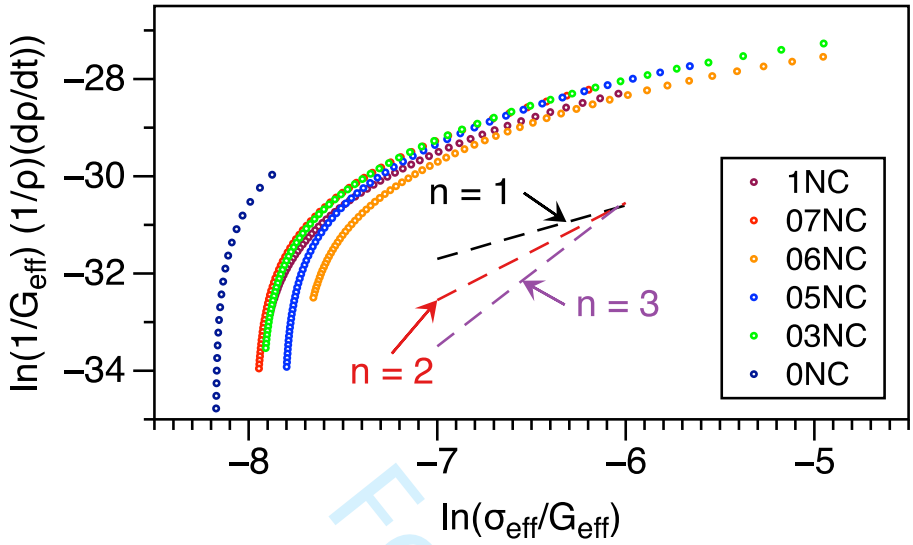

Figure S11. Analysis of the SPS of carbide in the TaC – NbC system at 2200 °C.

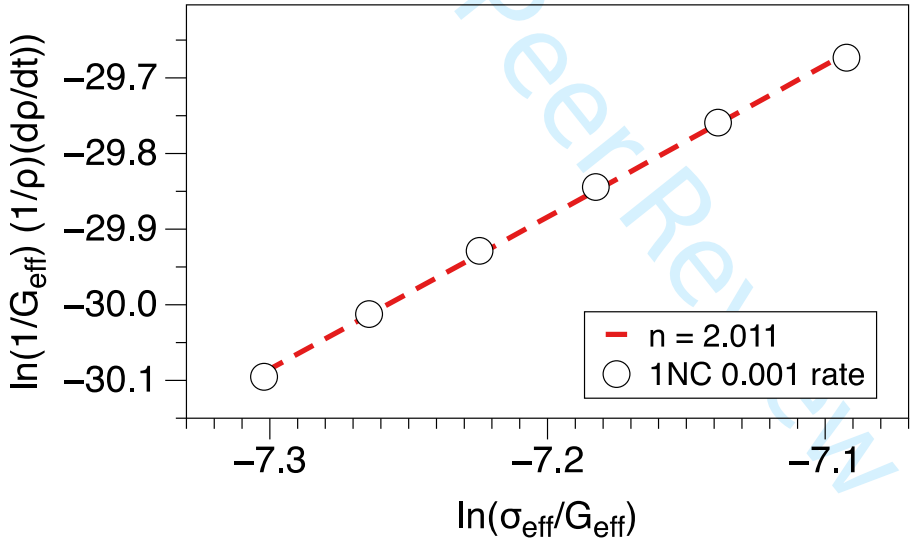

Figure S12. Analysis of the SPS of NbC at 2200 °C.

Table T2 Calculated values of stress exponents (*n*) for all compositions.

Composition NbC, mol.%	Temperature, °C	***n***	R^2
0	2200	5.3	0.83
30	2200	1.85	0.99
50	2200	1.45	0.89
66	2220	1.94	0.99
75	2200	1.76	0.97
100	2200	2.01	0.98
100	2100	1.87	0.97
100	2000	1.85	0.96

Supporting information, *S6. XRD results in the TaC–NbC system*

Figure S13 illustrates a full version of stacked plot for the XRD profiles collected in the TaC–NbC system. (b) is used in the manuscript.

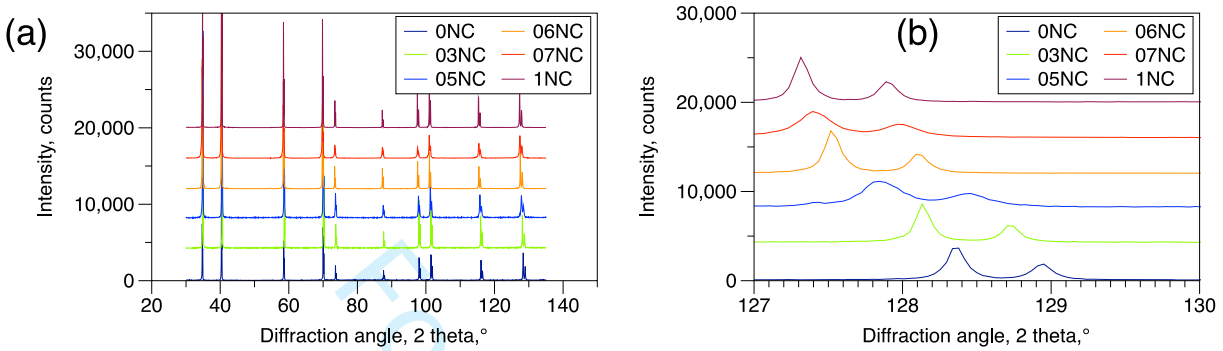

Figure S13. X-Ray diffraction profiles for SPSed ceramics in the TaC–NbC system.

P-13

Supporting information, *S7. Summary of fracture toughness trials for TaC*

Figure S14 illustrates toughness data collected for the monolithic tantalum carbide using a single edge through-thickness notch. One can see that using a a0/W ratio will provide a good consistency in the toughness value.

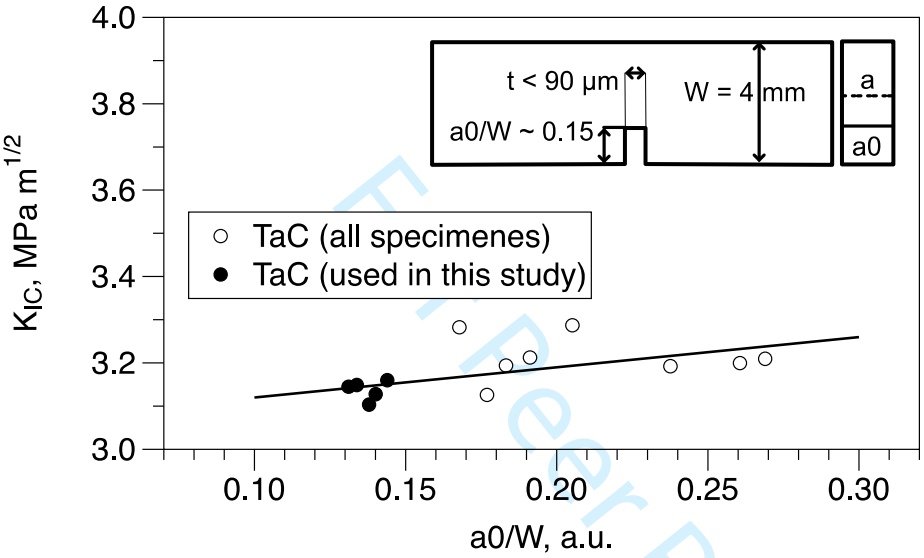

Figure S14. Effect of notch size (a0/W ratio) on K_{IC} for TaC determined on straight notch samples.

Supporting information, *S8. Typical secondary phases for the SPS ceramics*

Figure S15 and **S16** show the EDS profiles for the oxycarbide phases for ceramics in the TaC–NbC system. **Figure S16** in particular shows that alumina that was used during polishing can be entrapped in the pore and thus can be misinterpreted for the oxide phase. As a rule, oxygen for polished specimen was within 3 mol.%, and thus one may consider this as an absorbed oxygen during polishing.

For the analysis of the EDS data, we used NIST DTSA-II software [R8]. The spectra of the bulk TaC, NbC and equimolar solid-solution between these diborides made on specially prepared specimens served as a reference point in the analysis of the solid-solutions or oxycarbide phases. In order to verify the presence of oxides, the bulk Nb_2O_5 and Ta_2O_5 were also probed. Oxides were prepared by cold-pressing powders from Wako Pure Chemical Industries, Japan.

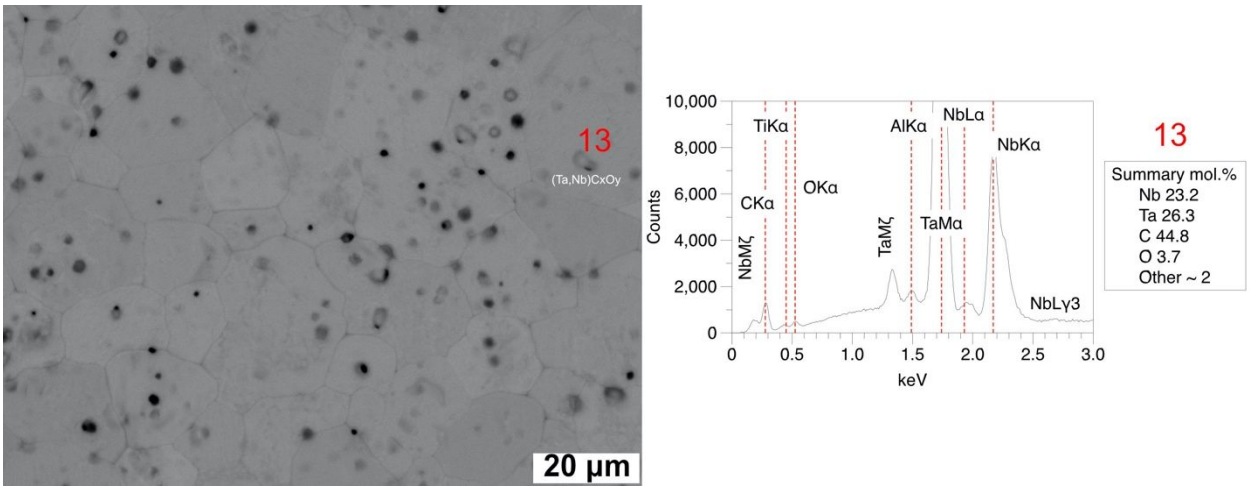

Figure S15. SEM micrograph of 50 mol.% NbC ceramic consolidated using the spark plasma method. This is a thermally etched surface acquired from the side of the bar after flexure at 1600 °C. (13) refer to EDX data from the spot analysis.

P-15

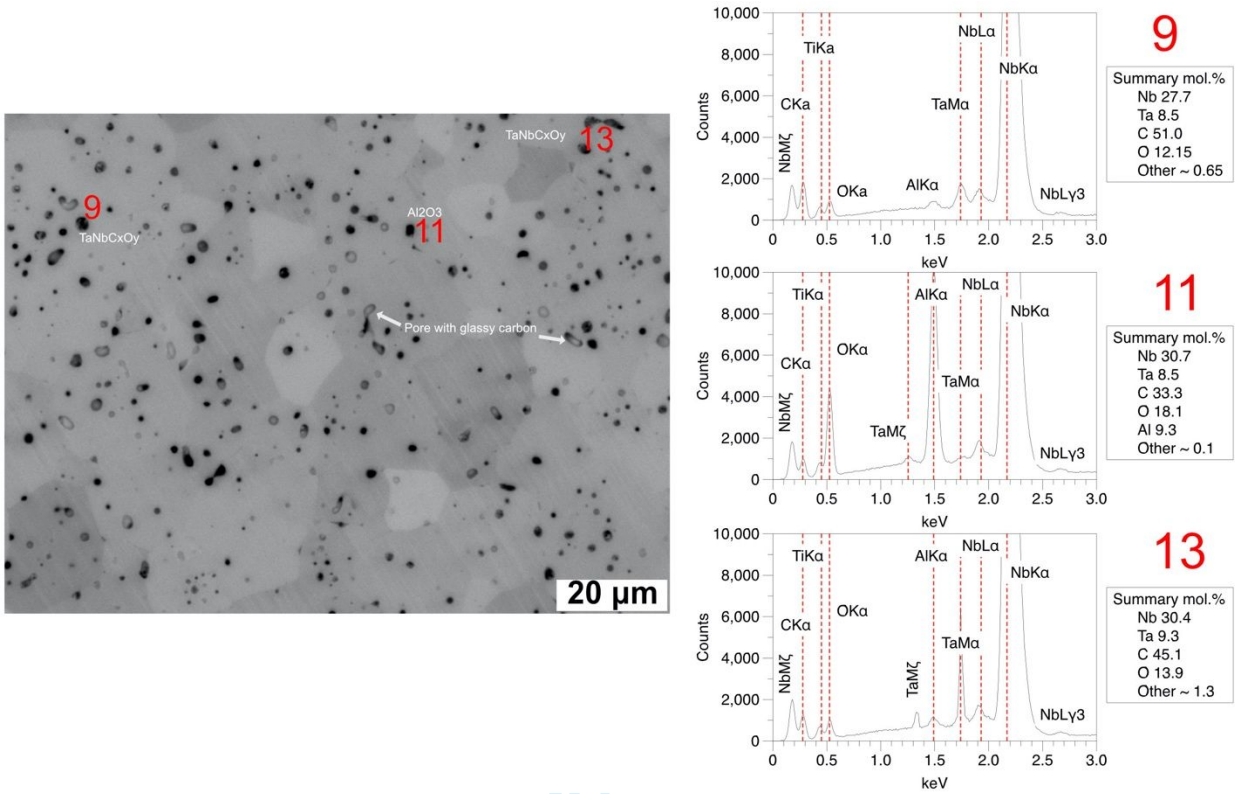

Figure S16. SEM micrograph of 66 mol.% NbC ceramic consolidated using the spark plasma method. (9),(11),(13) refer to EDX data from the spot analysis.

Supporting information, *S9. High-temperature creep for the binary carbides*

For other carbide systems such, as ZrC-TaC [R9] or HfC-TaC [R10], NbC-ZrC [R11], the clear maximum in the creep resistance or in the activation energy was previously reported, suggesting a contribution of the solid-solution strengthening to the high-temperature creep resistance. As it can be expected, this is also connected to the difference in the radii of the metal atom [R12].

Comparing the high-temperature flexural strength with the creep data, one can separate the data according to the **Fig. 13** as NbC-rich and TaC-rich. The NbC-rich solid-solution would retain a strength up to 1600 °C. After reaching this temperature the strength will linearly decrease with the temperature. For these ceramics, the loading rate had no clear effect on the yield strength or flexural strength, and importantly, only at 2000 °C were the typical plastic (sigmoidal) strain-stress curves observed.

At the same time, the 03N and 05N compositions showed a constant decrease in strength. The equimolar composition can be approximated using the exponential expression 226*exp(-232/(T+273)), suggesting that the defect flow in the crystal is quite sensitive to the temperature. Kelly and Rowcliffe [R13] reported for the monolithic TaC and NbC that the yield stress will have a similar temperature dependence only in the temperature range 1700–2050 °C. The temperature

dependence of the yield stress τ on the absolute temperature T can be expressed in the form

$\tau = \tau_0 \exp (E/RT)$,

where the τ_0 is a constant, R is the universal gas constant, and E is the apparent activation energy for the deformation process.

The majority of the carbides would have such a dependence only at the elevated temperatures [R14,R15]. However, it is unclear why the low-temperature zone can be approximated for the equimolar composition within this study. Most likely, this is a coincidence as the decrease in strength below 1200 °C can due to a number of factors already discussed including surface defects. For other ceramics within the studied NbC–TaC composition, such a decrease would be generally observed above 1800 °C, as is the contribution from the plastic deformation.

Other solid-solution systems featuring NbC and TaC, namely, the ZrC–TaC [57] and ZrC–NbC [R11] featured a clear maximum at 40 and 50 mol.% of the ZrC. As can be seen from the TaC–HfC data [R16], the equimolar solid solution can possess lower strength compared to other compositions at 2000 °C, as the maximum in the strength was near the 20 mol.% TaC ceramic. These facts may add an additional complexity to the analysis of the flexural strength dependencies.

References

[R1] Lanin A. Nuclear Rocket Engine Reactor. Berlin, Heidelberg: Springer; 2013.

[R2] Andrievski RA, Klymentko VV, Khromov YF. Self-diffusion of carbon in transition metal carbides of IV and V group. Phys Met Metallogr. 1969;28[2]:298–303.

[R3] Rafaja D, Lengauer W, Wiesenberger H. Non-metal diffusion coefficients for the Ta–C and Ta–N systems. Acta Mater. 1998;46[10]:3477–3483. doi:10.1016/S1359-6454(98)00036-6.

[R4] Rafaja D, Lengauer W, Wiesenberger H, Joguet M. Combined refinement of diffusion coefficients applied on the Nb-C and Nb-N systems. Metall Mater Trans. A 1998;29:439–446. doi: 10.1007/s11661-998-0124-z

[R5] Bernard-Granger G, Guizard C. Spark plasma sintering of a commercially available granulated zirconia powder: I. Sintering path and hypotheses about the mechanism(s) controlling densification. Acta Mater. 2007;44[10]:3493–3504. doi: 10.1016/j.actamat.2007.01.048.

[R6] Andrievski RA, Spivak II. Strength of Refractory Compounds. Chelyabinsk: Metallurgiya; 1989. (in Russian).

[R7] Helle AS, Easterling KE, Ashby MF. Hot-isostatic pressing diagrams: New developments. Acta Metall. 1985;33[12]:2163–2174. doi: 10.1016/0001-6160(85)90177-4.

[R8] Newbury DE, Ritchie NWM. Performing elemental microanalysis with high accuracy and high precision by scanning electron microscopy/silicon drift detector energy-dispersive X-ray spectrometry (SEM/SDD-EDS). J Mater Sci. 2015;50:493–518. doi: 10.1007/s10853-014-8685-2.

[R9] Kats SM, Ordan'yan SS. Extreme character of concentration dependence of creep rate of solid solutions of ceramics in the M^{IV}–$M^{V}C$ system. Izd Akad Nauk SSSR, Neorg Mat. 1983;19[2]:196–201.

[R10] Katz SM, Ordan'yan SS, Zaitsev GP. High-temperature creep in solid-solutions of the HfC–TaC system. Izd Akad Nauk SSSR, Neorg Mat. 1981;17[11]:2039–2043.

[R11] Avgustinik AI, Katz SM, Ordan'yan SS, Goryn AI, Kudryasheva LV. Compressive creep in ZrC–NbC solid-solutions at temperatures 2600–3150 °K. Izd Akad Nauk SSSR, Neorg Mat. 1972;7[8]:1417–1420

[R12] Kats SM, Ordan'yan SS. Creep in sintered polycrystalline niobium carbide and niobium carbide-based solid solutions. Powder Metall Met Ceram. 1984;23:414–418. doi: 10.1007/BF00796613.

[R13] Kelly A, Rowcliffe DJ. Deformation of Poly crystalline Transition Metal Carbides. J Am Ceram Soc. 1967;50[5]:253–256. doi: 10.1111/j.1151-2916.1967.tb15098.x.

[R14] Hollox GE. Microstructure and mechanical behavior of carbides. Mater Sci Eng. 1968;3[3]:121–137. doi: 10.1016/0025-5416(68)90001-3.

[R15] Kelly A, Rowcliffe DJ. Deformation of Poly crystalline Transition Metal Carbides. J Am Ceram Soc. 1967;50[5]:253–256. doi: 10.1111/j.1151-2916.1967.tb15098.x.

[R16] Demirskyi D, Borodianska H, Nishimura T, Suzuki ST, Yoshimi K, Vasylkiv O. Deformation-resistant Ta0.2Hf0.8C solid-solution ceramic with superior flexural strength at 2000°C. J Am Ceram Soc. 2022;105[1]:512–524. doi: 10.1111/jace.18072.